

Article

Drimia maritima as a New Green Inhibitor for Al-Si Alloy, SAE Steel and Pure Al Samples in 0.5 M NaCl Solution: Polarization and Electrochemical Impedance Analyses

Rodrigo S. Bonatti ¹, Diego Costa ² , Giovana S. Padilha ¹ , Ausdinir D. Bortolozo ^{1,2} and Wislei R. Osório ^{1,2,*} 

¹ Faculdade de Ciências Aplicadas, FCA, Centro de Pesquisa em Materiais Avançados (CPMMA), Campus II, Universidade de Campinas/UNICAMP, Limeira 13484-350, SP, Brazil; robonatti@yahoo.com.br (R.S.B.); giovanap@unicamp.br (G.S.P.); ausdinir@unicamp.br (A.D.B.)

² Faculdade de Tecnologia, FT, Campus I, Universidade de Campinas/UNICAMP, Limeira 13484-332, SP, Brazil; diegocosta54@gmail.com

* Correspondence: wislei1@unicamp.br

Abstract: The corrosion inhibition effects of *Drimia maritima* (L.) Stearn sin. *Urginea maritima* (L.) Backer on three different materials, i.e., as-cast Al-7 wt.% Si alloy, SAE 1020 low carbon steel, and commercially pure Al samples, into a stagnant and naturally aerated 0.5 M NaCl solution are evaluated. For this purpose, both the potentiodynamic polarization curves and electrochemical impedance spectroscopy with an equivalent circuit are utilized. It is found that inhibition effect increases up to certain minor *Drimia maritima* content. Adsorption isotherms (e.g., Langmuir and Temkin) indicate that all three examined materials comprise physical adsorption mechanisms. Al-Si alloys attained inhibition efficiencies of about 96% at 25 °C with 1250 ppm of *Drimia maritima* and ~43% with 625 ppm at 45 °C. On the other hand, the cp. Al and SAE 1020 samples attain ~89% and 68% with 1250 ppm and 500 ppm at 25 °C, respectively. This clearly indicates that the dosage of *Drimia maritima* green inhibitor into NaCl solution possesses certain susceptibility for each distinctive material examined. Impedance parameters obtained by using CNLS (complex non-linear least squares simulations) are correlated and discussed.



Citation: Bonatti, R.S.; Costa, D.; Padilha, G.S.; Bortolozo, A.D.; Osório, W.R. *Drimia maritima* as a New Green Inhibitor for Al-Si Alloy, SAE Steel and Pure Al Samples in 0.5 M NaCl Solution: Polarization and Electrochemical Impedance Analyses. *Metals* **2024**, *14*, 1147. <https://doi.org/10.3390/met14101147>

Academic Editor: Sebastian Feliú Jr.

Received: 28 August 2024

Revised: 2 October 2024

Accepted: 5 October 2024

Published: 8 October 2024



Copyright: © 2024 by the authors. Licensee MDPI, Basel, Switzerland. This article is an open access article distributed under the terms and conditions of the Creative Commons Attribution (CC BY) license (<https://creativecommons.org/licenses/by/4.0/>).

1. Introduction

Corrosion is a catastrophic deterioration of materials occurring due to electrochemical reactions, one of an anodic nature and the other cathodic [1–3]. This is provoked by the potential difference between the oxidant (generally the corrosive medium) and the anode (metal). The energy absorbed by the metal during its extraction is the “driving force” to achieve a stable oxidation state, considering that even temporarily, there is always a non-stable stage [3,4]. The corrosion of metals has a significant impact on the development of a country, contributing to direct and indirect financial losses. It is even compared to the costs related to any natural disaster like an earthquake [5]. Kesavan and collaborators [5] have reported that direct costs related to corrosion in the USA have reached about USD 276 billion per year. This is relatively higher than normalized losses computed from natural disasters (~USD 17 billion). It is also reported [5,6] that about 25 to 30% of annual corrosion costs can be prevented or managed by appropriate practices related to minimizing the phenomenon. Among various preventing mechanisms of the metallic corrosion, the corrosion inhibitors constitute one of these methods to minimize or eliminate the undesirable deterioration. In the same direction as the financial expenses related to the corrosion phenomena affecting the economy [5,6], the use of corrosion inhibitors also plays an important role in a country’s economy [7].

In a general and simplified way, the corrosion inhibitor is a compound or chemical substance [8–10], which is commonly added in minor quantity (up to 1% wt.%) [9–11]. These compounds are adsorbed on metal surfaces, and the corrosive effect is minimized. The effect of the inhibitor is usually evaluated by calculating its inhibition effectiveness, i.e., a percentage calculated between the relative corrosion in the medium containing and absenting content of the inhibitor compound.

Distinct inhibitors are widely used [7–9] such as cooling and water treatment systems in concrete and the handling and storage of electronic and military equipment [9–11]. It is recognized that the corrosion inhibitor efficiency is different inside the same industrial application. This is intimately associated with the diversity of environmental conditions, the nature of the industrial equipment, or the physiochemical characteristics of the water used in the system [9].

From the material behavior point of view, aluminum induces 100% recycling without considerable loss of its natural qualities. Sangeetha and collaborators [12] have reported that in Europe, among Al recycling fields, approximately 42% were related to “soda and beer cans”. In terms of corrosion, Al, in its pure state, does not have high corrosion resistance, especially considering its corrosion potential, when compared to other elements. However, since a thin oxide layer (e.g., Al_2O_3 , $\text{Al}(\text{OH})_3$, and $\text{AlO}(\text{OH})_2$) forms on its surface, it is highly resistant to corrosion in both air and in most environments [2,3,12–17]. On the other hand, in media containing chlorides or acidic media, the mentioned oxide layer is significantly affected.

Due to their rigidity combined with “lightweight” characteristics, aluminum alloys are adopted into automotive, aerospace, and aeronautical applications [1,14–16]. When Al is passivated, an oxide protective layer can be constituted. However, distinct Al-based alloys contain intermetallics [16], and these provoke substantial corrosion resistance decreasing [12–17]. Due to their high technological value and wide industrial application, both Al and its alloys represent an important category of material [17]. During the last 12 years involving various Al alloys (e.g., Al-Cu, Al-Si, Al-Zn, Al-Cu-Si, Al-Fe, Al-Ni, Al-Pb, etc.), it has been reported a close correlation between the resulting microstructural array and their corrosion resistance and mechanical properties [18–23].

Concerning corrosion inhibitors, Kesavan et al. [5] have reported that one of the first studies considering organic corrosion inhibitors is attributed to Speller and co-authors [5,24]. During several decades, chromates and nitrates, among others, were widely used. However, due to their toxic and carcinogenic aspects, a great number of other inhibitors without harmful effects have been focused on distinctive studies. Moreover, the “contaminant” or “non-natural” aspects and difficulties in disposing and packaging the compound produced open the way for fierce but corroborative exploration in “green chemistry”. This provides an opportunity to plan, to develop, and to create any research with a non-polluting aspect and with minimal production of waste/waste (disposal). In addition, it should be associated with minimum energy consumption [25].

Considering the aspects of cost, biodegradability, low toxicity, availability, and “environmentally friendly”, a new class of corrosion inhibitors emerges and is recognized as “green inhibitors” [26]. Obi-Egbedi and collaborators [26] have reported that certain organic inhibitors provide anticorrosive aspects, but they still possess certain toxicity [25–27]. These compounds still have a mixture of surfactant and/or solvent and also include polyphenols, terpenes, carboxylic acids, and alkaloids [8]. Depending on the portion, these have no environmentally friendly aspects. Additionally, it should be mentioned that a disadvantage of green inhibitors concerns their stability in the conditions tested. For instance, the polyphenol-based extracts are less toxic than alkaloid, but their stability is a drawback [8]. Moreover, another disadvantage concerns the extraction method, which can negatively affect the rate and yield of inhibition. Xhanari et al. [8] have reported a review paper demonstrating these organic inhibitors and their extraction routes with corresponding advantages and drawbacks.

Based on this, in a general way, the use of inhibitory molecules containing heterocyclic compounds with polar functional groups (e.g., N, S, O, and P) and associated with double bonds in different aromatic structures is preferred for the inhibition effect [25–27]. Basically, these substances adsorb on the metal surface, and the deterioration reaction is minimized or blocked [25].

Sangeetha et al. [12] have reported more than 20 different natural extracts from plants acting as green corrosion inhibitors for Al and alloys (e.g., Al-Mg, Al-Mg-Si, and Al-Zn-Mg) in distinctive corrosive media, e.g., NaCl, HCl, and NaOH. Inzunga et al. [9] have reported that since 1982, more than 44 patents on corrosion inhibitors considering heat exchangers containing water for protecting steel in concrete and the oil/petroleum industry were published. Xhanari and co-authors [8] point out that caring for the environment using sustainable and abundant sources has an important parameter of impact on society and the people's well-being. They have also shown a distribution and research carried out in the last 20 years related to natural plant extracts for use as corrosion inhibitors, intrinsically related to Al and its alloys [8]. In this work, 176 references are cited, of which more than 70% report on plant extracts and natural products (e.g., mango skin, coffee, pineapple, jasminum tea, hibiscus, ginseng, mint, among others). Medicines (when consumable by humans, e.g., the antibiotic amoxicillin), "gummies" (arabica and xantham), and natural oils (bee honey) complete the set of research on green corrosion inhibitors at work [8].

Badawi and Fahim [28] have shown that green corrosion inhibitors are classified as "organic-based" and "inorganic-based" (commonly from rare earth elements) compounds. From those organics are mentioned surfactants, plants, biopolymers, and amino acid substances. They have also suggested that organic-based compounds, loafs, fruits/vegetable peels, and roots are the majority utilized. Based on all referenced works and especially those that review the literature [8,9,12,13], it is clearly observed that the method and technique used to extract the inhibitor compound interfere with its efficiency, purity, concentration of inhibitor, and antioxidant activity. Furthermore, the extraction time and cycle, temperature, and solvents used (e.g., methanol, ethanol, isopropanol, acetone, acids, and ethyl acetate, among others) [8] present complexity, and expensive methods and techniques are involved. It is observed that literature is scarce concerning the interpretation of impedance parameters, mainly capacitance and resistances associated. Also, the equivalent circuits adopted provide limitations in their interpretation and correlation with the adsorption mechanism. This present study is focused on evaluation of the electrochemical impedance parameters associated with polarization results and correlating with the physio-chemical adsorption mechanisms of the proposed green inhibitor. Associated with this novelty, it is stated that a new green inhibitor is investigated. It is prepared from the *Drimia maritima* (L.) Stearn sin. *Urginea maritima* (L.) Backer [29–32], which has not been reported as a green corrosion inhibitor. It is remarked that a very simple extraction route is adopted, i.e., natural products are immersed into distilled water and inhibitors are easily obtained. It is a plant native to the Mediterranean region, Africa, and India [32]. Based on its content molecule, it is reported that it provides positive effects in respiratory deficiency treatments (e.g., as pneumonia, bronchitis, and asthma) [32]. This substance also has anti-inflammatory, antioxidant, and antibacterial effects. Due to the presence of bufadienolide glycoside compounds, it has been clinically used to treat cardiac disorders based on proscillarin A [33], which is one of the most important constituents [32,33] when a gel from the plant is obtained. It is also worth highlighting that activity antitumor (e.g., human lymphoma [34], breast cancer [35,36], human fibroblasts, adrenocortical carcinoma, etc.) was also investigated for this type of compound obtained mainly from *D. maritima* [33].

It is remembered that contributions in this investigation concern the simple and cheap extraction method to obtain a green inhibitor. Also, its inhibition efficiency is evaluated by using three different materials widely applied in distinct industrial sectors. With this, an as-cast Al-Si (Al-7.5% wt.% Si alloy), a commercially pure Al sample (as-cast), and a sample of SAE 1020 low-carbon steel are evaluated.

2. Experimental Procedures

2.1. Materials: Natural Green Inhibitor

The plant (*D. maritima*) is also known as sea onion, *Scilla maritima*, and yellow onion, among other ones. It belongs to the *Liliaceae* family, grows from autumn to spring and has a certain ornamental value. It produces flowers, but the compound under investigation is found in the bulb, being part of the research interest of the species [29–36]. There are two species; one is white and the other red [29], which is attributed to the preparation of rodenticides [29–32]. A viscous white to clear liquid is withdrawn from bulbs. A gel is produced by mixing 1:1 from viscous liquid with distilled water (pH = 6.98 (± 0.02) (at environmental temperature, $\sim 25 \pm 2$ °C). It is remarked that it is not added other compounds or solvents for its extraction, e.g., methanol, ethanol, acids, salts, or acetone [8,30,31,37–39]. Moreover, no heating is used, as widely reported. Summarizing, the extraction of natural inhibitor is immersing “sea onion” into a portion of distilled water, and green inhibitor is easily obtained.

To effectively prepare the gel, the bulbs are washed. After, the bulbs are cut using clean and sterilized utensils to avoid possible contamination. The portion of bulb is added to distilled water and kept for 24 h. After this period, the “gel” is constituted, and for each distinct material, determined portions into stagnant 0.5 M NaCl (electrolyte) at a temperature of about 25 (± 2) °C are used. The inhibition effects of *Drimia maritima* or sea onion as a green inhibitor for Al-Si alloy, SAE 1020, and c.p. (commercially pure) Al samples are investigated.

2.2. Materials: Alloys and Electrolyte Solution

In order to evaluate the inhibition effects added to aggressive medium (NaCl solution), three distinct materials are used: Al-7.5% wt.% Si alloy (AS); c.p. Al ingot (AP); and SAE 1020 low carbon steel (CS). Although there is a great gamma of materials with diverse applications, these materials were selected based on their possible applications in the aerospace and automotive industries, heat exchangers, water treatment systems, etc. [1,18–23,40,41]. A volume of about 40 (± 2) mL of a stagnant and naturally aerated 0.5 M NaCl (electrolyte solution) at environmental temperature (25 ± 2 °C) is used. The inhibition effect by using Al-Si alloy at 45 (± 3) °C is also adopted to confirm the decreasing protection effect, as expected for the majority or all inhibitors. The metallic samples (i.e., AS, AP, CS) with areas of about 1 (± 0.3) cm² were prepared for electrochemical measurements. Before all electrochemical tests, the samples were adequately ground by using commonly sequenced SiC papers up to 1200 grit SiC papers. These samples constitute the working electrode (WE).

2.3. Electrochemical Measurements and Inhibitor Efficiency (IE)

A conventional system of three-electrode cell kits is used to evaluate the corrosion behavior. The WE with specific exposed area is constituted by different materials (AS, AP, CS), while a platinum plate (~ 1000 mm²) and a saturated calomel electrode (SCE) constitute the counter and reference electrodes. A volume of about 40 (± 2) mL of a stagnant and naturally aerated 0.5 M NaCl (electrolyte solution) at environmental temperature (25 ± 3 °C) is used.

Before each experimentation, the samples are immersed until a steady state is reached ($\sim 15 \pm 2$ min). VersaStat 4, Princeton Applied Research® (PAR) (Wokingham, UK) is used. Electrochemical impedance spectroscopy (EIS) measurements are carried out prior to potentiodynamic polarization tests. EIS initiates after steady state, and sequentially, polarization measures are carried out. EIS measures are carried out using 10 points per decade with an amplitude potential of about 10 mV, peak-to-peak (AC signal) in open circuit, and a frequency range between 10⁵ Hz and 10⁻² Hz is adopted. CNLS (complex non-linear least squares) simulations are carried out to compare simulated data with those experimental results. For this, ZView® software (version 2.1b), Scribner Association Inc., Southern Pines, NC, USA, is used and associated with an equivalent circuit (EC)

and obtained the data. The EC is shown when EIS data are shown and discussed. The potentiodynamic polarization measurements are carried out considering an open-circuit potential with a determined scan rate of 0.167 mV/s from -600 to -1000 mV (vs. SCE) is selected. All experimentations are carried out at least considering duplicates in order to guarantee their reproducibility.

The inhibitor efficiencies, i.e., IE(i) and IE(R), are calculated in percentages as described in Equations (1) and (2). These consider the corrosion current densities (i_{corr}) obtained from the potentiodynamic polarization curves and the polarization resistance (R_2) parameters obtained from EIS data/simulation CNLS, respectively.

$$IE(i)\% = \left(\frac{i_{corr}^{(blank)} - i_{corr}^{(inh)}}{i_{corr}^{(blank)}} \right) \times 100 \quad (1)$$

$$IE(R)\% = \left(\frac{R_2^{(blank)} - R_2^{(inh)}}{R_2^{(blank)}} \right) \times 100 \quad (2)$$

where $i_{corr}^{(blank)}$ and $i_{corr}^{(inh)}$ are the obtained values of the corrosion current densities without “green inhibitor” content and by using distinctive concentrations (i.e., 150, 300, 625, 1250, and 1875 ppm) of the *Drimia maritima* gel as green inhibitors. Analog $R_2^{(blank)}$ is the resistance associated with a determined capacitance in the absence of the green inhibitor content, and $R_2^{(inh)}$ corresponds to polarization resistance associated with distinct concentration contents. Both resistances are obtained from EIS parameters when fitting experimental data using CNLS simulation.

2.4. Adsorption Isotherms Determinations

In order to determine the interaction between inhibitor molecule and surface of the examined metal (i.e., Al, Al alloy, and SAE low carbon steel), the adsorption isotherms are determined. These help to understand or to prescribe the mechanism of adsorption. Langmuir isotherm, modified Langmuir, Temkin, Frumkin, Flory–Huggins, and Freundlich isotherms are used. Based on the attained correlation coefficients (R^2) provided by each one of the isotherms, the quality fitting is achieved, and the adsorption behavior profile is discussed. Equations and other details corresponding with distinct isotherms are forwardly provided and discussed. Associated with each selected isotherm, the adsorption coefficient (K) and the standard Gibbs free energy of adsorption (ΔG_{ads}) are also determined and forwardly discussed.

3. Results and Discussion

Before initiating the discussion, it is important to remember that a transparent gel from the bulb of *D. maritima* is obtained and used as a potential green inhibitor. For this purpose, Al-7.5 wt.% Si alloy, c.p. Al, and SAE 1020 samples are examined. Same areas and similar conditions (stagnant 0.5 M NaCl) to corrosion measurements are used. These materials are adopted since they are commonly used in a great variety of industrial applications. Additionally, with these materials, a general visualization for potential utilization of *D. maritima* as a green inhibitor is provided. Interestingly, no alcohol route or distillation or synthesizing route using solvent is applied. A simple aqueous extraction is carried out. Although there exist some limitations in the present investigation, the results indicate that a new and promising green inhibitor is attained.

3.1. Chemical Constituents of *Drimia maritima* Bulbs

It is important to remark that in this present investigation neither gas chromatography-mass spectroscopy (GC-MS) nor FT-IR spectra results are carried out. The CG-MS results are based on a recent investigation reported by Al-Abdallat [42]. They have published a phytochemical analysis of *D. maritima*. The analysis according to NIST 20 and Willy 19 Libraries [42] has revealed fifty-seven (57) compounds as its composition. Although a

great quantity of constituents is detected, six (06) compounds constituting higher quantities are remarked and shown in Table 1. It is observed that “Campesterol” constitutes ~14% of the total. The other two compounds have ~10% each one, i.e., 2,3-Butanediol and 5-Hydroxymethylfurfural. Moreover, the fatty acids designated as “Hexadecanoic acid ethyl ester” and “9-Octadecenamide (Z)-” constitute ~8% for each one.

Table 1. Main compounds detected in *Drimia maritima* bulbs using aqueous extraction. Percentages are obtained from GC-MS [42]. (*) Data obtained from www.sigmaldrich.com, accessed 10 April 2024).

| Compounds | Common Name | % | Formula (*) | Structure (*) | Density (g/mol) * | Number of Atoms |
|--------------------------------|----------------|-------|--|---------------|-------------------|-----------------|
| Campesterol | phytosterol | 13.87 | C ₂₈ H ₄₈ O | | 400.69 | 77 |
| 2,3-Butanediol | glycol/alcohol | 10.45 | C ₄ H ₁₀ O ₂ | | 90.12 | 16 |
| 5-Hydroxymethylfurfural | -- | 9.85 | C ₆ H ₆ O ₃ | | 126.11 | 15 |
| 9-Octadecenamide | Oleamide | 8.14 | C ₁₈ H ₃₅ NO | | 281.48 | 55 |
| Hexadecanoic acid, ethyl ester | Palmitic acid | 8.05 | C ₁₈ H ₃₆ O ₂ | | 284.48 | 56 |
| Proscillarin A | -- | 4.96 | C ₃₀ H ₄₂ O ₈ | | 530.67 | 80 |

As expected, all organic compounds have a long carbon chain with a great number of atoms and relatively complex molecular structures. Intending to propose the adsorption mechanisms to metals proposed (Al-Si alloy, c.p. Al, and SAE 1020 carbon steel), these complex molecular structures involve certain difficulty in a schematic representation depicting the exact point or electronic region of a particular molecule or a partial region evidencing its chemisorption or physisorption process. Based on this, a representative green “molecule” compound will be considered, as will be depicted. It is worth noting that all these identified compounds are commercialized (e.g., Sigma-Aldrich) and are relatively expensive when individualized synthesized (e.g., proscillarin A and campesterol are relatively expensive, i.e., ~USD 800.00 per 10 mg).

3.2. Al-Si Alloy Results

3.2.1. Potentiodynamic Polarization Measurement

The results are organized in three distinct materials, i.e., Al-Si alloy, c.p. pure Al, and SAE 1020. Based on this organization, the discussion initiates with the Al-Si alloy containing its corresponding potentiodynamic polarization curves, followed by the electrochemical impedance spectroscopy (EIS), adsorption isotherm data, and its tentative explanation of the mechanism of inhibition.

Figure 1a depicts the resulting potentiodynamic polarization (PP) curves of as-cast Al-7.5 wt.% Si alloy in a stagnant and naturally aerated 0.5 M NaCl solution at environmental temperature (25 ± 3 °C). The Tafel’s method is used to obtain i_{corr} with absence and containing five distinct concentrations of the *D. maritima*, i.e., 150, 300, 625, 1250, and 1875 ppm. Additionally, a supersaturating or overdosage of inhibitor is used in order to demonstrate there is no inhibitor after a certain dosage or concentration. From here, the green inhibitor is designated as “DRIMIA” to facilitate its nomenclature in discussion sections. The inhibition efficiencies based on the corrosion current densities, IE(i)% , are

determined according to Equation (1), as previously described. The surface coverage (θ) values are also determined based on Equation (1), considering the absolute value.

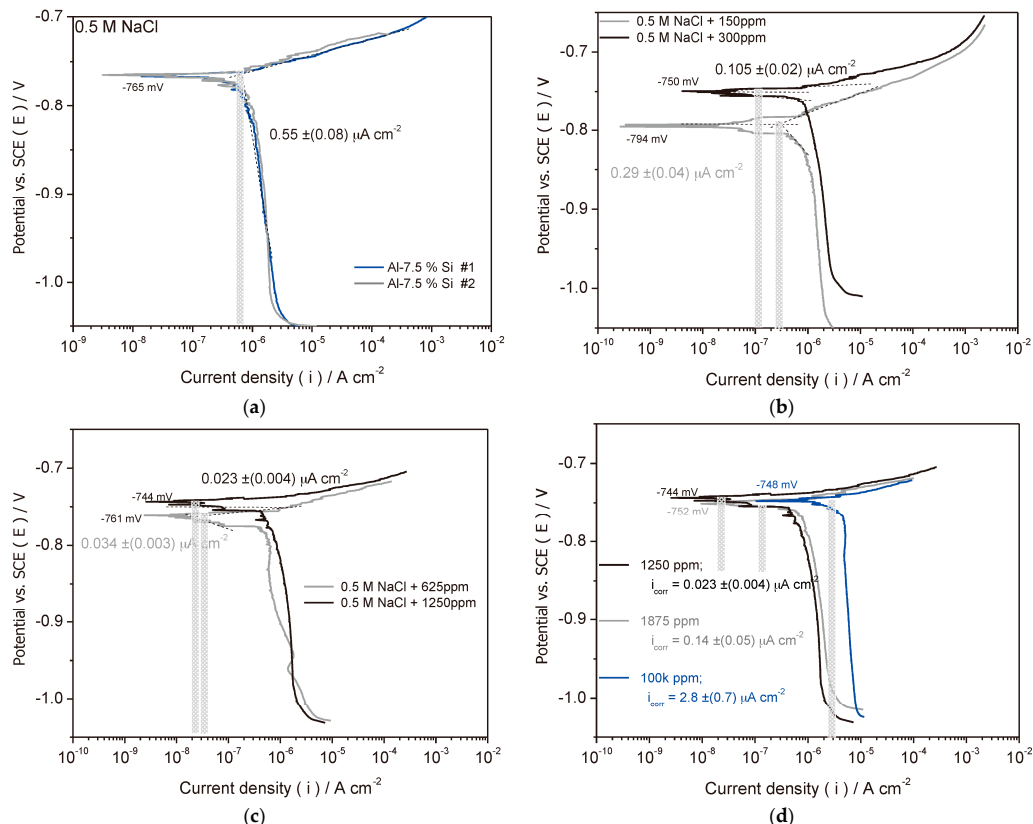


Figure 1. Experimental results of the potentiodynamic polarization curves of the as-cast Al-7.5 wt.% Si alloy in a stagnant and naturally aerated 0.5 M NaCl solution at environmental temperature ($25 \pm 3^\circ\text{C}$): (a) with absence of inhibitor *D. maritima*, (b) with 150 and 300 ppm, (c) containing 625 and 1250 ppm, and (d) showing 1250, 1875, and 100,000 ppm.

Figure 1b shows PP curves of Al-7.5 wt.% Si (Al-Si) alloy also immersed into a stagnant and naturally aerated 0.5 M NaCl (40 mL) containing distinct DRIMIA contents, i.e., 6 mL and 12 μL added into 40 mL of electrolyte (0.5 M NaCl). With these two distinctive concentrations depicted, i.e., 150 and 300 ppm, respectively. Figure 1c,d depicts the resulting PP curves of the Al-Si alloy sample with three different DRIMIA contents, i.e., 625, 1250, and 1875 ppm, respectively. Although it is observed that 1875 ppm (i.e., 75 μL in 40 mL of DRIMIA) provides a reasonable decrease in the corrosion inhibition, a supersaturated concentration of 4000 $\mu\text{L}/40$ mL was soaked, and its deleterious effect was observed.

Qualitative analyses among the obtained PP curves reveal that in the examined samples with DRIMIA contents, the cathodic plateau tends to decrease. Associated with this, it is clearly observed that with the increase of green inhibitor content, the i_{corr} decreases. This is verified up to 1250 ppm, as observed in Table 2. Both the IE(i)% and θ are also demonstrated in Table 2. It is remarked that from those error ranges of the i_{corr} , the average values for all examined samples are considered. It is also important to remark that Tafel's extrapolations are obtained using both anodic and cathodic branches, and no substantial modifications in the slope of the experimental curves are verified. This seems to confirm that no mixed inhibitor behavior is prevalent, which can occur in some cases. The cathodic branches corresponding with the sample containing 625 ppm (Figures 1c and 2b) depict a slight oscillation close to -950 mV (SCE), which was not clearly verified in other ones. However, it is not assured or stated that a distinctive and substantial phenomenon as a mixed behavior is occurring. Moreover, this has not affected the determination of the Tafel extrapolation or the determination of the corrosion current density.

Table 2. Parameters obtained from the potentiodynamic polarization (PP) curves of Al-Si alloy immersed into a 0.5 M NaCl solution with absence and distinctive *Drimia maritima* contents at $25 (\pm 3)^\circ\text{C}$ and the calculated inhibition efficiency percentage (IE%) and surface coverage (θ).

| Concentration (ppm) | i_{corr} ($\times 10^{-6} \text{ A/cm}^2$) | Ecorr (mV) | IE% | θ |
|---------------------|--|------------------|-------------|-------------|
| Blank | 0.550 (± 0.08) | -765 (± 2) | - | - |
| 150 | 0.290 (± 0.04) | -794 (± 2) | 47.3 | 0.47 |
| 300 | 0.105 (± 0.02) | -750 (± 2) | 80.9 | 0.81 |
| 625 | 0.034 (± 0.003) | -761 (± 2) | 93.8 | 0.94 |
| <u>1250</u> | 0.023 (± 0.004) | -744 (± 2) | 95.8 | 0.96 |
| 1875 | 0.140 (± 0.05) | -752 (± 2) | 74.5 | 0.75 |
| 100k | 2.798 (± 0.7) | -748 (± 2) | N/C | N/C |

N/C = no coverage attained. Bold and underline means the highest IE and surface coverage.

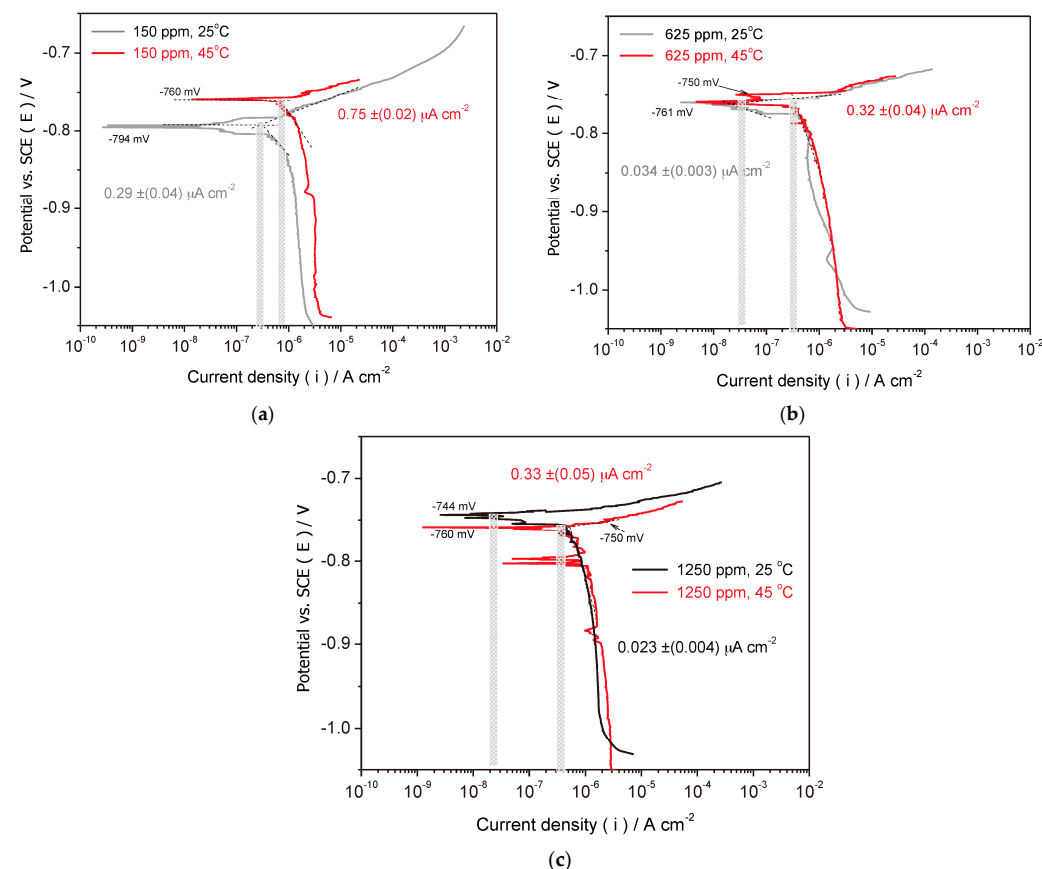


Figure 2. Experimental results of the PP curves of the as-cast Al-7.5 wt.% Si alloy in a stagnant and naturally aerated 0.5 M NaCl solution comparing results at $25 (\pm 3)^\circ\text{C}$ and $45 (\pm 3)^\circ\text{C}$ in different concentrations: (a) 150 ppm, (b) 625 ppm, and (c) 1250 ppm.

The highest corrosion inhibition is attained when 1250 ppm of DRIMIA content is applied. Their inhibition efficiency is $\sim 96\%$. This means that the absolute value of i_{corr} has decreased $\sim 24\times$ when compared with the blank sample. Although a concentration of 1875 ppm is lower $\sim 4\times$ than the blank, it substantially decreases ($\sim 6\times$) their inhibition when compared with the sample soaked with 1250 ppm of DRIMIA. When a supersaturation of the DRIMIA content is applied (i.e., 100k ppm), it is confirmed that a corrosion inhibitor is absent. A drastic corrosion action is provoked, i.e., the i_{corr} severely increases by $5\times$ when compared with the blank, and both the IE and θ are not determined. These results indicate that there exists a limit dosage (in ppm) of the proposed green corrosion inhibitor.

To confirm this possible inhibition, three concentrations are selected to be performed using heating solution, i.e., at $45 (\pm 3)^\circ\text{C}$.

Figure 2a–c shows comparisons between results of potentiodynamic polarization (PP) curves of the Al-Si alloy in a stagnant and naturally aerated 0.5 M NaCl solution at $25 (\pm 3)$ and $45 (\pm 3)^\circ\text{C}$ in three distinct *Drimia maritima* concentrations, i.e., containing 150, 625, and 1250 ppm, respectively. It is evidenced that at 45°C , the inhibition corrosion efficiency is drastically decreased when compared with the results at 25°C . However, with 626 and 1250 ppm, the inhibitions provided at 45°C are achieved and slightly lower than the blank, i.e., 0.31 and 0.35 against $0.55 \times 10^{-6} \text{ A/cm}^2$. Also, it seems that the high temperature provokes a high level of oscillations in cathodic branches and a slightly higher plateau in cathodic with anodic branches, suggesting that at about -750 mV an abrupt “film breaking”, which was not observed when examined samples were subjected to 25°C . This suggests a different “protection film formation” and its breaking and/or distinct absorption mechanism. However, no pitting potential is analyzed, and these aforementioned assertions are speculative, and a systematic experimentation should be carried out. From this moment, it is only noticeable that slight differences in shapes of PP curves are observed. Forwardly, when the EIS parameter is discussed, the adsorption mechanism will be analyzed.

Table 3 clearly demonstrates that at 45°C both the inhibition efficiency (IE) and surface coverage (θ) are substantially decreased when compared with the same concentration at 25°C . When hot temperature is considered, the corrosion inhibition (i.e., ~between 40 and 42%) reaches a plateau between 625 ppm and 1250 ppm. If error ranges are considered, it can be said that similar inhibition efficiencies are attained. However, it is slightly suggested that 1250 ppm is the limiting and certain degradation starts to be involved. With this, it is hardly suggested that at hot temperatures the DRIMIA content must obligatory be evaluated to attain a reasonable protection level.

Table 3. Parameters obtained from the curves of Al-Si alloy immersed into a 0.5 M NaCl solution at $25 (\pm 3)$ and $45 (\pm 3)^\circ\text{C}$ and the calculated inhibition efficiency percentage (IE%) and surface coverage (θ).

| Concentration (ppm) | icorr (25°C) ($\times 10^{-6} \text{ A/cm}^2$) | icorr (45°C) ($\times 10^{-6} \text{ A/cm}^2$) | IE% (25°C) | θ | IE% (45°C) | θ |
|---------------------|---|---|----------------------------|----------|----------------------------|----------|
| 150 | 0.290 (± 0.04) | 0.75 (± 0.02) | 47.3 | 0.47 | N/I (*) | --- |
| 625 | 0.034 (± 0.003) | 0.32 (± 0.04) | 93.8 | 0.94 | 41.82 | 0.42 |
| 1250 | 0.023 (± 0.004) | 0.33 (± 0.05) | 95.8 | 0.96 | 40.00 | 0.40 |

(*) → N/I = no inhibition provided at this temperature and concentration.

Although it is difficult to compare these results with previously reported considering Al alloys, it is accepted or recognized that hot temperature decreases the inhibition effect. The difficulty to compare is associated with different nature of electrolyte, e.g., acidified or alkalinized, material of substrate examined, and characteristic/nature of the inhibitor.

For instance, it was researched that some similar corrosion inhibitors for Al alloys and degradation of their inhibition at high temperatures were achieved, but no articles were achieved. However, for instance, Rugmini Ammal et al. [37] have investigated the corrosion inhibition effect of HMATD (i.e., 4-(4-hydroxy-3-methoxy benzylidene amino)-4-H-1,2,4-triazole-3,5-dimethanol) on mild steel in a 0.5 M HCl solution. They have shown that the highest IE at 30°C and at 45°C is achieved by using the same HMATD concentration (300 ppm). In another investigation [38] using Al alloy and green corrosion inhibitor (*Spondias mombin* L.) immersed in a 0.5 M H_2SO_4 solution, the authors have also found that the highest IE values at 30 and 60°C are provided by the same concentration.

Wang et al. [39] have also found the highest IEs with the same green inhibitor concentration at different temperatures (20, 30, 40, and 50°C). Evidently, in all three aforementioned studies, certain degradation levels are observed when a hot temperature is applied when compared with a colder (less warm) temperature. It seems that with the increase in temperature, the DRIMIA inhibitor content should be revised and adjusted to the new level

of temperature applied. This seems to constitute a limitation to the hot application of this kind of inhibition. Probably this seems to correlate with the adsorption mechanism, i.e., physisorption or chemisorption. This will forwardly be discussed.

3.2.2. Electrochemical Impedance Spectroscopy (EIS) Measurements

In order to provide more details concerning the electrochemical behavior of the Al-Si alloy samples, EIS results are organized and discussed. Figure 3 shows Bode, Bode-phase, and Nyquist plots with their corresponding fittings by using CNLS simulation and an equivalent circuit. It is remarked that EIS measurements are carried out before polarization. However, it adopted its presentation after PP due to the more level of details provided.

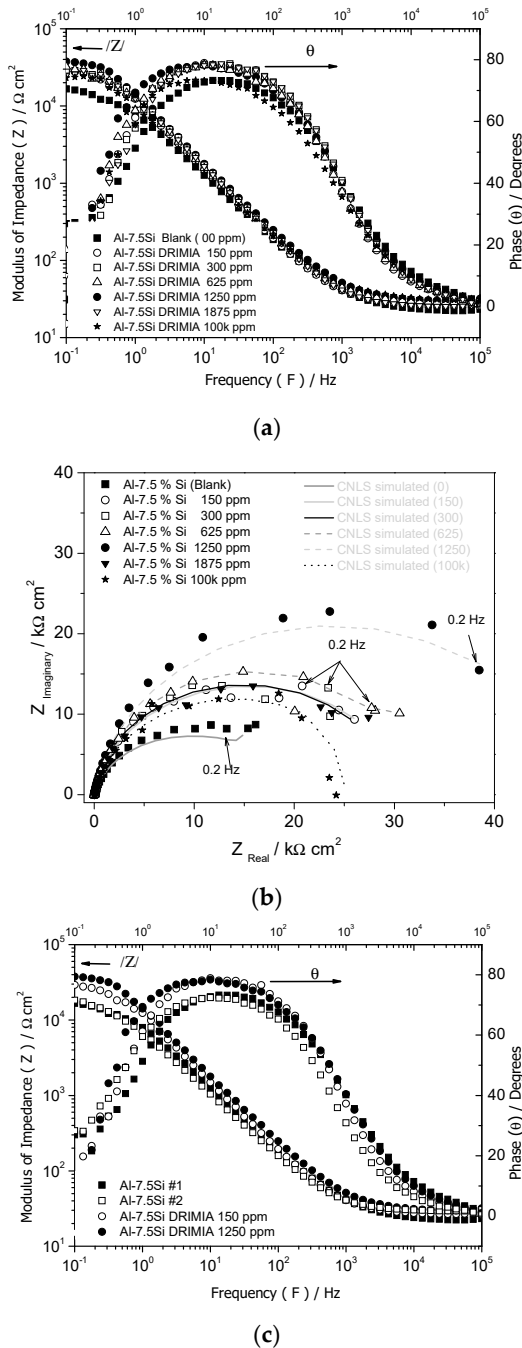


Figure 3. Cont.

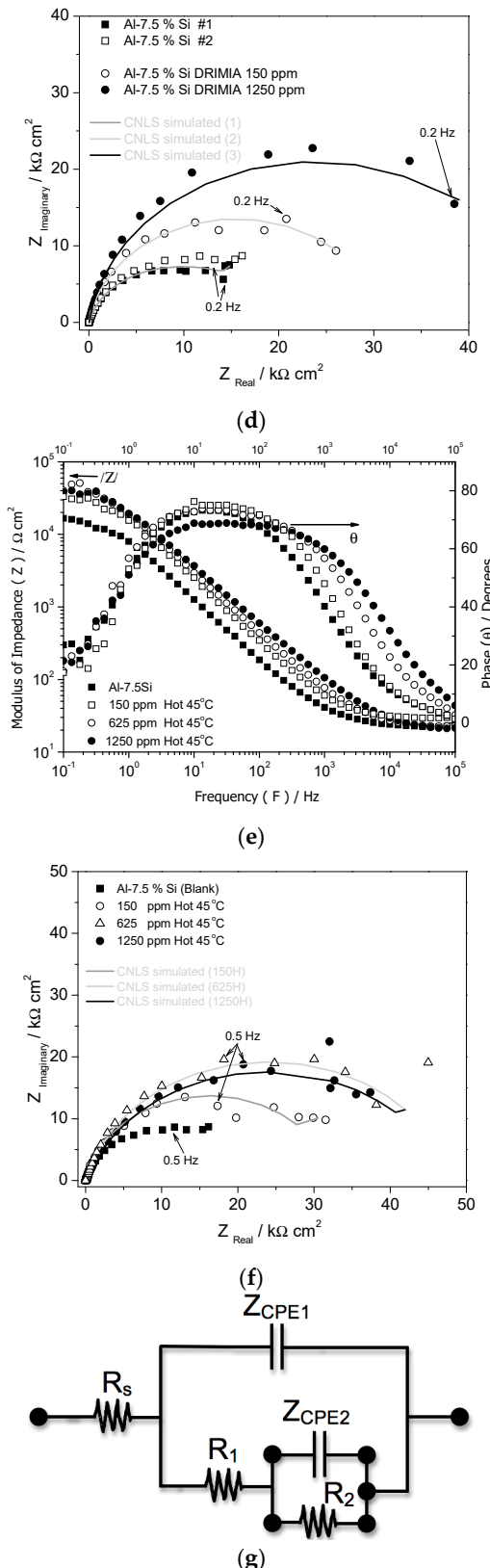


Figure 3. Experimental EIS results of the Al-7.5 wt.% Si alloy in 0.5 M NaCl solution: (a) Bode and Bode-phase plots, (b) Nyquist diagrams comparing blank with distinctive concentrations, (c) and (d) showing duplicate for blank, and 150 and 1250 ppm comparisons, respectively; and (e,f) comparison among EIS plots of blank and 150, 625, and 1250 at 45 °C, also in a 0.5 M NaCl; and (g) the proposed equivalent circuit to obtain data EIS parameters using CNLS simulations.

Figure 3a,b depicts the resulting Bode and Bode-phase plots and Nyquist plots of Al-Si in a stagnant and naturally aerated 0.5 M NaCl at 25 (± 3) °C with the absence and containing distinctive concentrations of *Drimia maritima* (DRIMIA). In a rapid qualitative analysis of these EIS plots, it is clearly perceived that the DRIMIA provides corrosion inhibition. However, as also revealed by experimental PP curves, this inhibition has a certain limit, i.e., up to 1250 ppm. When 1875 ppm and a super dosage of DRIMIA (100k ppm) are utilized, the modulus of impedance ($|Z|$) and phase angle decrease. This suggests that inhibition efficiency is negatively affected. Quantitative analyses are provided when impedance parameters are obtained by using CNLS simulations. It is important to observe that EIS plots have similar format/shape with absence and containing inhibitor contents. Figure 3c,d also demonstrates experimental results of Bode and Bode-phase plots and Nyquist plots of the Al-Si alloy, but only depicting duplicate results for Al-Si with the absence of inhibitor and the other two containing 150 and 1250 ppm. This is to facilitate the visualization of the main results when compared with Figure 3a,b with all data depicted.

Figure 3e,f shows the experimental results of the Bode and Bode-phase plots and Nyquist plots of the Al-Si alloy in a stagnant and naturally aerated 0.5 M NaCl solution at 45 (± 3) °C, considering also three inhibitor concentrations, i.e., 150 ppm, 625 ppm, and 1250 ppm. When a qualitative comparison is made, EIS plots reveal slight differences in shapes. Nyquist plots have semi-arcs decreased and a Bode/Bode-phase diagram, although with similar slopes, these are slightly dislocated to the right side with increasing inhibitor content. Analog occurrence is also verified for the Bode-phase curves, mainly in the high-frequency domain (i.e., between 10^3 and 10^5 Hz). This is also associated with a slight decrease in the maximum phase angles, which are decreased and also dislocated to the right side. These observations suggest lower corrosion protection when compared with samples examined at 25 °C. Thus, it is indicated that hot temperature has a deleterious effect on the inhibition efficiency. This discussion is quantitatively provided when the impedance parameters are obtained using the equivalent circuit (EC) as proposed in Figure 3g. By using EC, the CNLS simulations provide good quality fitting between experimental and simulated data, as prescribed by the obtained parameter designated as chi-squared (χ^2). With the EIS parameters, a quantitative discussion concern to electrochemical corrosion and inhibition behavior can be provided. These values are shown in Table 4, as follows.

The proposed equivalent circuit (EC) is suggested due to EIS plots indicating two time constants. Although it was not necessary to determine the number of time constants, a method [40,41,43,44] is proposed in the literature. Based on similar curves of all examined samples in EIS plots, it was adopted that two constants domain the electrochemical behavior of all examined samples. The physical significance of R_s is the resistance of the electrolytic solution (0.5 M NaCl). R_1 and R_2 represent the resistances of charge transfer of the at-surface and intermediate regions containing the inhibitor molecule, possibly interacting with intermediate corrosion by-products and adsorbed intermediate products, respectively. Moreover, the elements $Z_{CPE(1)}$ and $Z_{CPE(2)}$ represent the capacitances associated with the inner and outer film layers on the surface of the Al-Si alloy, respectively. The parameter Z_{CPE} characterizes the impedance of a phase element, as in Equation (3).

$$Z_{CPE} = [C(i\omega)^n]^{-1} \quad (3)$$

where C is the capacitance; i is the current (imaginary number: $-1^{0.5}$); ω is the angular frequency, and $-1 \leq n \leq 1$ [43,44]. A CPE with $n = 1$ represents an ideal capacitor, and when $0.5 < n < 1$, a distribution of relaxation times in the frequency space is represented.

Based on the EIS parameters shown in Table 4, considering experimentations with absence (blank) and containing distinctive inhibitor concentrations in a 0.5 M NaCl solution at 25 °C, it can be observed the modifications attained. For instance, R_s very slightly increases (i.e., ~22 to 31) with the increase in the inhibitor content. However, this increase is not substantial to predict a different ohmic resistance of the electrolyte to conclude that certain molecules or partial ions have been dissolved and modified significantly the resistance of the electrolyte.

Table 4. Experimental impedance parameters of the Al-Si alloy in 0.5 M NaCl solution with distinctive DRIMIA contents by using CNLS simulation and equivalent circuit.

| Parameters (at 25 °C) | Blank | 150 ppm | 300 ppm | 625 ppm | 1250 ppm | 1875 ppm |
|--|---------------------------|----------------------------|---------------------------|---------------------------|---------------------------|---------------------------|
| Rs ($\Omega \cdot \text{cm}^2$) | 22 (± 0.4) | 27 (± 0.3) | 27 (± 0.5) | 29 (± 0.5) | 29 (± 0.5) | 31 (± 0.5) |
| $Z_{\text{CPE}1}$ (10^{-6} F/cm^2) | 4.49 (± 0.2) | <u>10.6</u> (± 0.05) | <u>8.8</u> (± 0.8) | <u>10.2</u> (± 0.3) | <u>8.4</u> (± 0.5) | <u>10.9</u> (± 0.3) |
| R_1 ($\Omega \cdot \text{cm}^2$) | 28 (± 6) | <u>196</u> (± 19) | <u>320</u> (± 80) | <u>240</u> (± 40) | <u>293</u> (± 45) | <u>228</u> (± 50) |
| n_1 | 0.97 | 0.93 | 0.94 | 0.92 | 0.92 | 0.91 |
| $Z_{\text{CPE}2}$ (10^{-6} F/cm^2) | 1.94 (± 0.2) | <u>3.62</u> (± 0.5) | <u>2.69</u> (± 0.3) | <u>3.74</u> (± 0.3) | <u>3.58</u> (± 0.8) | 6.29 (± 0.5) |
| R_2 ($10^3 \Omega \cdot \text{cm}^2$) | 19.2 (± 0.3) | <u>29.3</u> (± 0.4) | <u>30.6</u> (± 0.5) | <u>34.7</u> (± 0.7) | 47.1 (± 0.7) | 27.6 (± 0.8) |
| n_2 | 0.80 | 0.91 | 0.94 | 0.90 | 0.92 | 0.91 |
| χ^2 | 4.31×10^{-3} | 2.54×10^{-3} | 2.54×10^{-3} | 3.26×10^{-3} | 4.91×10^{-3} | 16×10^{-3} |
| Sum of Sqr. | 0.41 | 0.23 | 0.23 | 0.30 | 0.44 | 0.98 |
| Parameters (at 45 °C) | Blank | 150 ppm | 300 ppm | 625 ppm | 1250 ppm | 1875 ppm |
| Rs ($\Omega \cdot \text{cm}^2$) | | 29 (± 0.5) | | 29 (± 0.2) | 21 (± 0.5) | |
| $Z_{\text{CPE}1}$ (10^{-6} F/cm^2) | | 7.92 (± 0.3) | | 7.34 (± 0.2) | 8.49 (± 1.1) | |
| R_1 ($\Omega \cdot \text{cm}^2$) | | 445 (± 62) | | 490 (± 80) | 1429 (± 240) | |
| n_1 | | 0.89 | | 0.86 | 0.81 | |
| $Z_{\text{CPE}2}$ (10^{-6} F/cm^2) | | <u>1.93</u> (± 0.3) | | <u>1.96</u> (± 0.2) | <u>1.05</u> (± 0.5) | |
| R_2 ($10^3 \Omega \cdot \text{cm}^2$) | | <u>31.9</u> (± 0.6) | | 46.7 (± 1.2) | 46.2 (± 0.8) | |
| n_2 | | 0.89 | | 0.86 | 0.83 | |
| χ^2 | | 3.31×10^{-3} | | 1.91×10^{-3} | 1.51×10^{-3} | |
| Sum of Sqr. | | 0.30 | | 0.18 | 0.14 | |

Underlined values indicate same range or order of magnitude and bold suggest better results.

On the other hand, it is clearly observed that R_1 and $Z_{\text{CPE}(1)}$, which should be together analyzed, are in the same order of magnitude for all samples containing inhibitor contents, i.e., R_1 between 200 and $300 \Omega \cdot \text{cm}^2$ and $Z_{\text{CPE}(1)}$ between 8 and $10 \mu\text{F}/\text{cm}^2$, excepting the sample with 1875 ppm. When R_2 and $Z_{\text{CPE}(2)}$ corresponding with inhibition contents are analyzed, it is revealed that the capacitances of $Z_{\text{CPE}(2)}$ are of the same magnitude (between 2.5 and $3.5 \mu\text{F}/\text{cm}^2$) and R_2 increases with the increase in the inhibitor content (i.e., from ~ 29 k to ~ 47 k $\Omega \cdot \text{cm}^2$), again excluding the sample with 1875 ppm. With these results, two main conclusions can be drawn. First, it is the fact that there exists the same configuration or nature of adsorption for all examined samples with inhibitor content. Secondly, and a slightly more complex and extensive explanation, is the fact that R_1 and $Z_{\text{CPE}(1)}$ seem to associate with the outer layer configured when the samples are in electrolyte solution immersed. Since R_1 values are lower than R_2 , it is indicated that lower “protection” energy is involved. This suggests that physical adsorption is prevalent. On the other hand, due to its highest values, it is suggested that R_2 is associated with higher “protection” energy and inhibition efficiency than R_1 , possibly involving the inner complex layer (due to complex intermediates), and associated with a chemical adsorption (chemisorption) mechanism. Since physisorption commonly involves relative weak intermolecular forces between metal and adsorbed molecule and chemisorption summarily involves substituting reactions between the surface of metal and adsorbed substance, it is suggested that R_1 and R_2 are predominantly associated with physisorption and chemisorption mechanisms, respectively. In addition, when $Z_{\text{CPE}(1)}$ and $Z_{\text{CPE}(2)}$ are evaluated, the former are around 8 and $10 \mu\text{F}/\text{cm}^2$ and the latter is lower ($\sim 3 \times$) than the former (i.e., 2.5 and $3.5 \mu\text{F}/\text{cm}^2$). Associated with the decreased capacitance, their corresponding resistance is increased, which is, from the electrochemical point of view, an indication that their electrochemical behavior is improved.

When the EIS parameters corresponding with the hot electrolyte (at 45 °C) containing inhibitor contents are analyzed, similar electrochemicals are verified at 25 °C, however, with decreased inhibition efficiency, as expected and also reported in the literature for all other kinds of inhibitors [37–39]. Thus, R_1 values ($\sim 450 \Omega \cdot \text{cm}^2$) are lower than R_2 ($\sim 450 \Omega \cdot \text{cm}^2$) and (between 30k and 45k $\Omega \cdot \text{cm}^2$). However, it is remarked that with 1250 ppm of DRIMIA

inhibitor, the inhibition efficiency starts its degradation or fade-out in protection is prevalent. Although its capacitance and resistance seem to indicate better results, it is worth noting that polarization curves previously analyzed have revealed similar behavior. Moreover, it should be mentioned that parameters “ n_1 ” and “ n_2 ”, which are lower than their peers, when 150 and 625 ppm are evaluated. Also, these parameters at hot electrolytes are lower than the environmental temperature. It remembered that “ n_1 ” and “ n_2 ” possibly reflect certain “unevenness” or irregularities on the electrode surface due to more complex intermediate formation and interaction of adsorption, as also reported by Wang et al. [39]. A lower value suggests more irregularities on the surface and more distant form ideal capacitor behavior, indicating a decrease in corrosion resistance or decreased inhibition efficiency. Since a great number of involved substances constitute the bulk of DRIMIA (with 57 distinctive substances), it is difficult to predict the accurate mechanism of adsorption. However, a tentative to prescribe this mechanism is proposed based on the experimental results obtained when isotherm adsorption analyses are carried out, as follows.

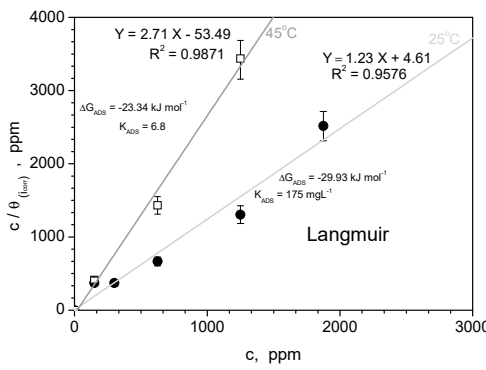
3.2.3. Adsorption Isotherm and Inhibition Activity Results

The understanding of the adsorption behavior of DRIMIA on the surface of Al-Si alloy is essential to explain its corrosion inhibition mechanism and facilitate the correlation with EIS and polarization parameters obtained. The inhibition efficiency (IE) determined by using corrosion current density is used to calculate the coverage θ , as shown in Tables 2 and 3. Based on these values and comparing or trying to compare with previous investigations, as also reported by Lai et al. [45], that recently concatenate some information concerning the inhibition efficiencies (IE) of different corrosion “organic” inhibitors for alloys in distinctive media. For instance, they [45] reported that IE of 93.3%, 94%, and 94.5% are attained when green inhibitors of Cassava starch graft copolymer (CSGC) [46], Konjac glucomanan (KGM) [47], and its owner inhibitor CPT (chitosan and 4-pyr-idinecarboxaldehyde) [45] are used, respectively. They [45] have stated that the IE found for CPT (i.e., 94.5%) is better than those already reported inhibitors used for aluminum alloy. It is really agreed with the authors that IE reached a substantial inhibition level. However, it is relatively complicated to compare with other studies. This is due to the fact that Al alloys present different solute content, which can infer galvanic couples and significantly affect the corrosion behavior. Moreover, each different study has considered a distinct medium. When CSGC is evaluated, HNO_3 solution is utilized, and when KGM is investigated, a NaCl solution is adopted, but a different Al alloy is used.

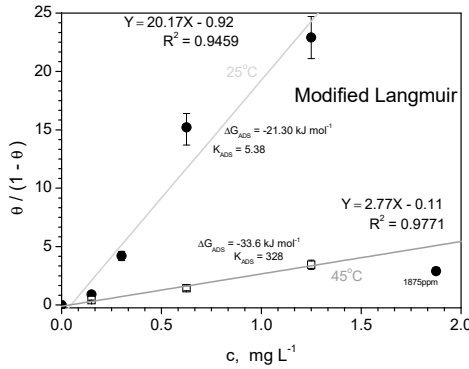
In addition to these comparisons provided by Lai et al. [45], four other studies involving green or eco-friendly inhibitors are included. The first dating into 2012 [38], reporting Spondias mombin L extract in sulphuric acid with an IE of 95.1%, and the second study published in 2019 [46], also involving green inhibitors for Al alloys immersed in HCl solution and reaching an IE of 95.6%. A third study published by Jakeria et al. [47] in 2022 involves an organic inhibitor (2-mercaptopbenzimidazole, 2MBI) on AA6061 Al alloy in 0.1M NaCl solution and an IE of about 65% after 1 day of immersion and ~20% after 14 days of immersion. A 4th investigation [48] recently published (at 2023) concerns the effect of rosemary extract in a 0.05 M NaCl solution in AA5052 Al alloy, and an IE of 96.48% is attained.

It is clearly observed that all aforementioned studies provide very acceptable IE levels. In our present study by using DRIMIA, the IE levels are about 95.8%, which is very compatible with those previously reported. This inhibition efficiency is reached when i_{corr} values are considered. When the polarization resistances (i.e., $R_1 + R_2$) obtained from the impedance parameters (shown in Table 4) are used, the IE percentages are reasonably distinctive (i.e., 34.9%, 37.9%, 45%, 59.5%, and 30.9%) from those calculated using i_{corr} values. However, the same trend is attained, i.e., increasing inhibition concentration; the highest IE is that of 1250 ppm (59.5%). Probably, these differences in the IE from i_{corr} and $R_1 + R_2$ are correlated with the equivalent circuit adopted.

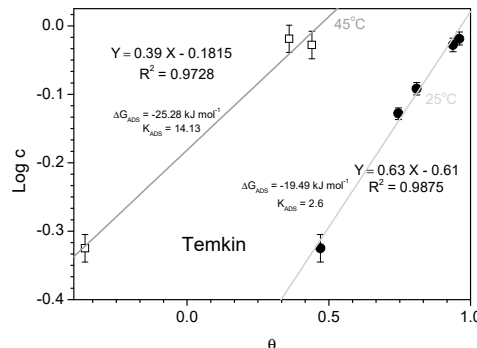
It is recognized that adsorption isotherms are utilized to prescribe the mechanism of adsorption and interaction between the inhibitor molecule and the Al surface (substrate). In this sense, there exists a great number of distinctive isotherm equations. Although commonly Langmuir isotherms or modified Langmuir equations are widely utilized, it was also tried to apply or calculate the inhibition efficiencies with other isotherms, such as modified Langmuir, Temkin, Frumkin, Flory–Huggins, and Freundlich isotherms, as shown in Figure 4. Based on the correlation coefficients (R^2) utilized to decide to adopt or to adjudge the isotherm providing best quality fitting, it is verified that Langmuir, modified Langmuir, and Temkin isotherms provide R^2 coefficients higher than 0.90, as depicted in Figure 4a–c, respectively. On the other hand, when utilizing isotherms of Frumkin, Flory–Huggins, and Freundlich isotherms, all obtained R^2 are lower than 0.90, which indicates these are not adequate to prescribe the adsorption behavior profiles. It is also remarked that Figure 4a–c also depicts isotherms considering experimentation at 45 °C, which also reveal R^2 with acceptable quality fitting, i.e., 98, 95, and 97%, respectively. Since other isotherms have not provided at 25 °C a good fit, no fit at 45 °C is used. Equations corresponding with distinct isotherms are widely reported [36–39,45–49].



(a)



(b)



(c)

Figure 4. Cont.

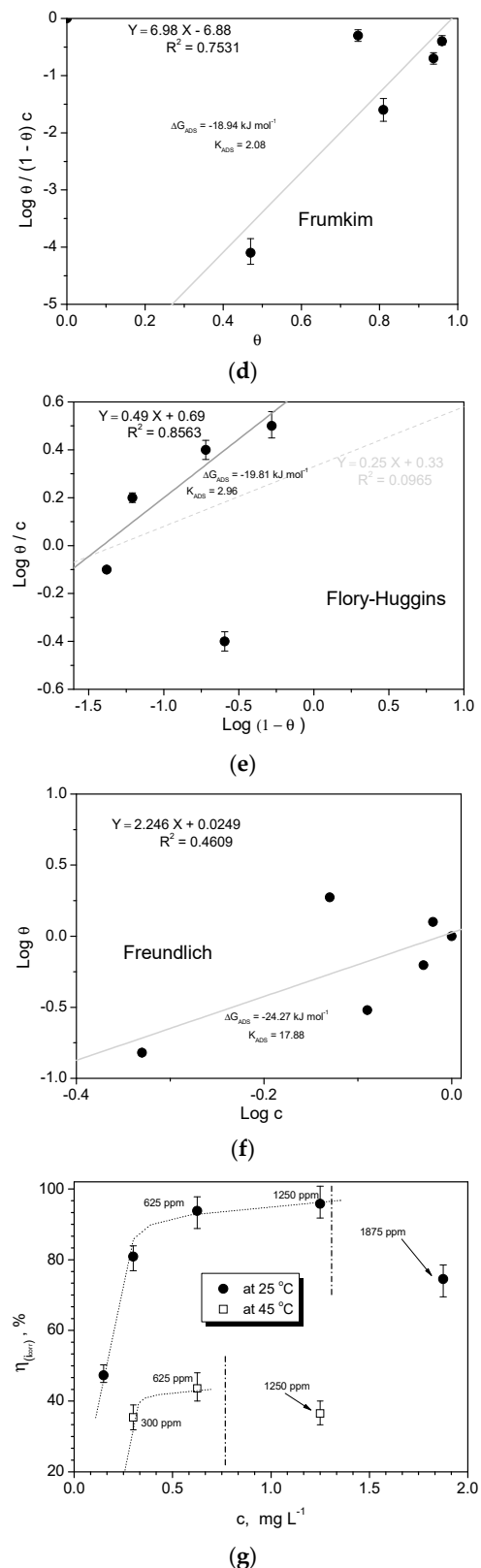


Figure 4. Langmuir (a) Langmuir modified (b), Temkin adsorption isotherm plots at 25 and 45 °C; (c,d) Frumkim, (e) Flory–Huggins and (f) Freundlich isotherm plots at 25 °C; and (g) inhibition efficiency (in percentages) with a function of the DRIMIA concentration at 25 and 45 °C.

Since Langmuir and Temkin isotherms provide the highest R^2 at both 25 and 45 °C, their corresponding equations are reported as Equations (4) and (5):

$$\frac{c}{\theta} = \left(\frac{1}{K} \right) + c \quad (4)$$

$$\exp(-2a\theta) = Kc \quad (5)$$

where θ represents the degree of surface coverage considering corrosion current densities (icorr) (Table 3), which are intimately associated with inhibition efficiency (IE). The inhibitor concentration or content is represented by “ c ”, in ppm; “ K ” (ppm⁻¹) is the equilibrium adsorption constant; and “ a ” is the molecular interaction parameter [49].

Figure 4a depicts “ c/θ ” versus “ c ” plot at 25 °C and 45 °C considering Langmuir isotherm. From the intercepts of the straight lines on these plots, the adsorption coefficient (K), which is related to the standard Gibbs free energy of adsorption designated as ΔG_{ads} , is determined by Equation (6).

$$\Delta G_{ads} = -R T \ln(10^6 K) \quad (6)$$

where R is the gas constant, T is the absolute temperature, and 10^6 is the concentration of water (mg/L) [45]. All ΔG_{ads} values are shown in Figure 4 (inset). It is recognized that negative ΔG_{ads} indicate a possible spontaneous and strong interaction adsorption of the extract on the Al surface is occurring [39,45]. Commonly, ΔG_{ads} close to -20 kJ mol⁻¹ or lower indicates consistent with the electrostatic interaction between charged organic molecules and the charged metal surface (physisorption). On the other hand, when close to -40 kJ mol⁻¹ or higher, it is suggested that the charge sharing or transfer from the organic molecules to the metal surface constituting a coordinate type of bond (chemisorptions) is provided [39]. Based on Figure 4 and all ΔG_{ads} values obtained, it is suggested that physical adsorption mechanism is prevalent, as also observed by Obi-Egbedi [38] when investigating *Spondias mombin* L. extract (organic inhibitor) on Al surface immersed in a 0.5 M H₂SO₄ solution. Farag et al. [49] have also observed a prevalent physical adsorption using an eco-friendly inhibitor for carbon steel in a 0.5 M H₂SO₄ solution.

Based on this, it seems that in all experimentations carried out using DRIMIA as an organic and eco-friendly corrosion inhibitor, a prevalent electrostatic interaction (physisorption) mechanism domains the adsorption between negatively charged DRIMIA components (are 57 compounds, as shown in Table 1) and positively charged cations of Al³⁺ at the surface. The inhibition efficiency (IE) as a function of DRIMIA concentration is shown in Figure 4g. It is clearly observed that the highest IE is attained with 1250 ppm, and increasing this content, a deleterious effect is prevalent, as aforementioned when discussing polarization and EIS parameters.

It is also suggested in the literature [45] that the IE depends on the applied temperature. The experimental results also indicate that at 45 °C, a decrease in the adsorption strength between the Al surface and inhibition molecules is observed, which suggests a physisorption behavior. Pradityana et al. [50] have stated that possibly electronegative O or N atom electron pairs and metal provide a nonpolar nature to organic inhibitors blocking the polar of corrosion solutions. This behavior is a physisorption mechanism between functional groups in the inhibitor molecule and metal.

Evidently, it is recognized that the chemical structure of the inhibitor molecules affects the inhibitor corrosion behavior due to the nature and charge of the metal. In this sense, although it is suggested that the predominant inhibitor mechanism is physisorption, with Al³⁺ favoring adsorption of Cl ions on its surface, the DRIMA molecules will stick onto the chloride ion adsorbed on the Al surface by physical adsorption. However, as also reported by Lai et al. [45], it seems that a non-predominant chemical adsorption can also occur. This is due to coordination bond formation among the lone pair electrons on the adsorption center (e.g., N and O, and empty orbitals of aluminum atoms).

Figure 5 shows a schematic representation suggesting a potential corrosion inhibition mechanism provided by DRIMIA when Al is immersed in a NaCl solution. Although a great number of compounds constitute the “macro molecule” of DRIMIA, the five main compounds (Table 1) are constituted by OH^- , heteroatoms N, O, and NH_2 , which can be adsorbed on the anionic sites and prevent hydrogen evolution, as similarly reported [39,48]. Although a molecular dynamic simulation has not been carried out (due to more complex compounds constituting the DRIMIA molecule), it is also suggested that a chemical adsorption between the heteroatoms (O) and Al atoms through electron transfer can also occur, as reported by Wang et al. [48]. It is remarked that predominant chemical adsorption domains the inhibition mechanism, as previously discussed and based on the adsorption parameters. Independently of the metal as substrate interacting with corrosive medium and containing DRIMIA content, it seems that this mechanism is also prevalent. In the next sections, SAE1020 steel and c.p. Al samples are also utilized to verify the possible inhibition behavior provided by DRIMIA molecules.

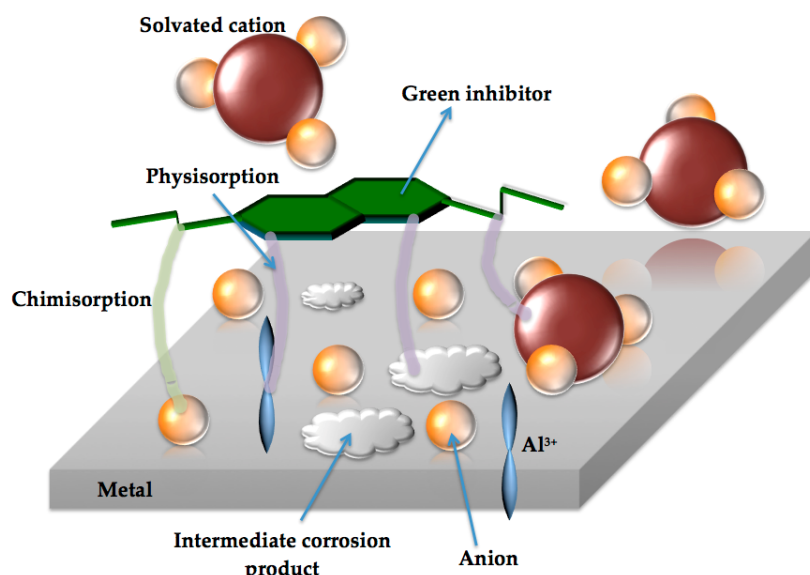


Figure 5. A schematic representation of the inhibition behavior provided by DRIMIA (*D. maritima*) over a Al-Si alloy in NaCl solution. Hypothetical interactions between heteroatoms of DRIMIA compounds (physisorption) with Al and solvated cation, intermediate complex corrosion by-product (physisorption); and inhibitor with anion at surface of metal (chemisorption).

3.3. SAE Steel and Commercially Pure Al Sample Results EIS and Potentiodynamic Polarization (PP) Measurements

As aforementioned, both SAE 1020 steel and c.p. Al samples are also experimented in NaCl solution containing DRIMIA contents. No systematic results are provided because it is only intended to verify a general inhibition effect of DRIMIA on these two materials. In this sense, only some certain concentrations are adopted. In Figure 6a–c, the experimental Bode and Bode-phase, Nyquist, and polarization curves (PP) obtained in a 0.5 M NaCl solution at environmental temperature are demonstrated.

Based on the EIE diagrams of the SAE 1020 steel samples, it is possible that the highest inhibition effect is reached when using 500 ppm of the gel. This indication is based on both the profiles characterized by the impedance moduli ($|Z|$) and phase angles (θ) and on the semi-arc profiles shown in the Nyquist plots, as depicted in Figure 6a,b, respectively. It is found that the gel containing DRIMIA compounds provides a considerable reduction in corrosive action.

Figure 6c shows the experimental results of PP curves of the SAE 1020 steel samples in 0.5 M NaCl. From those two (02) different levels of inhibitor contents examined, the inhibition effect is evident for both concentrations. However, using a 500 ppm content, the

inhibition effect is more effective, which indicates a better inhibition efficiency (η or IE). An IE of ~68% is attained when considering the corrosion current density value (i_{corr}) for the SAE 1020 sample without inhibitor, which is about $0.98 \times 10^{-6} \text{ Acm}^{-2}$. On the other hand, when a 500 ppm is used, the i_{corr} is of about $0.31 \times 10^{-6} \text{ Acm}^{-2}$, which is $\sim 3.2 \times$ lower than the blank sample. When 1500 ppm of inhibitor is considered, although still providing a reduction in i_{corr} (i.e., $0.55 \times 10^{-6} \text{ Acm}^{-2}$ versus $0.98 \times 10^{-6} \text{ Acm}^{-2}$), the percentage of the effective inhibition achieves approximately 44%. From the corrosion potential values verified into PP curves, it is also clearly observed that the addition of 500 ppm favors the potential to be shifted to more noble regions (fewer negative values), i.e., -655 mV (ESC). By using the concentration of 1500 ppm, an intermediate value is attained for the E_{corr} , i.e., -687 mV (ESC), when the sample without the inhibitor and at 500 ppm (i.e., -709 mV , ESC) is compared. These values and the i_{corr} values demonstrate the same sequence or tendency when the EIE diagrams are analyzed.

Figure 6d–f shows the experimental results of the c.p. Al samples in Bode and Bode-phase diagrams, Nyquist plots, and polarization curves (PP) in a 0.5 M NaCl solution at 25 °C. Comparing the Al samples (c.p.) containing 1250 ppm and without inhibitor compound, it is identified that an inhibition effect is provided. This suggests that the DRIMIA compound as a green corrosion inhibitor is a promising eco-friendly inhibitor. The Bode and Bode-phase plots indicate larger impedance modulus ($|Z|$) values associated with the phase angle (θ) values. Moreover, higher capacitive semi-arcs shown in the Nyquist diagrams (Figure 6e) indicate that DRIMIA (with 1250 ppm) provides a decrease in corrosive action. This corroborates the quantitative results obtained from the PP curves shown in Figure 6f. It is clearly observed that in the presence of the inhibitor DRIMIA in the saline solution, the i_{corr} decreases of about $10 \times$ while maintaining the corrosion potential in the same level or range (i.e., close to -730 mV , ESC). The corrosion inhibition efficiency (IE) attains 89.28% with a content of 1250 ppm.

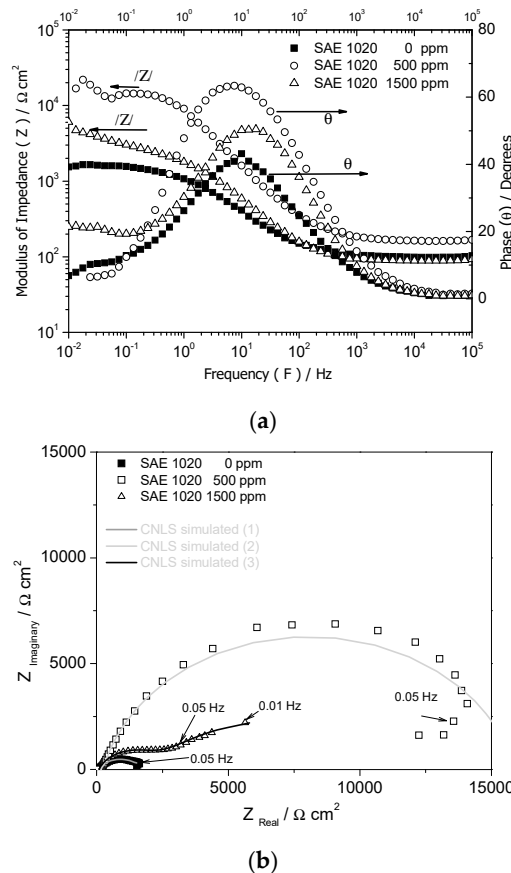


Figure 6. Cont.

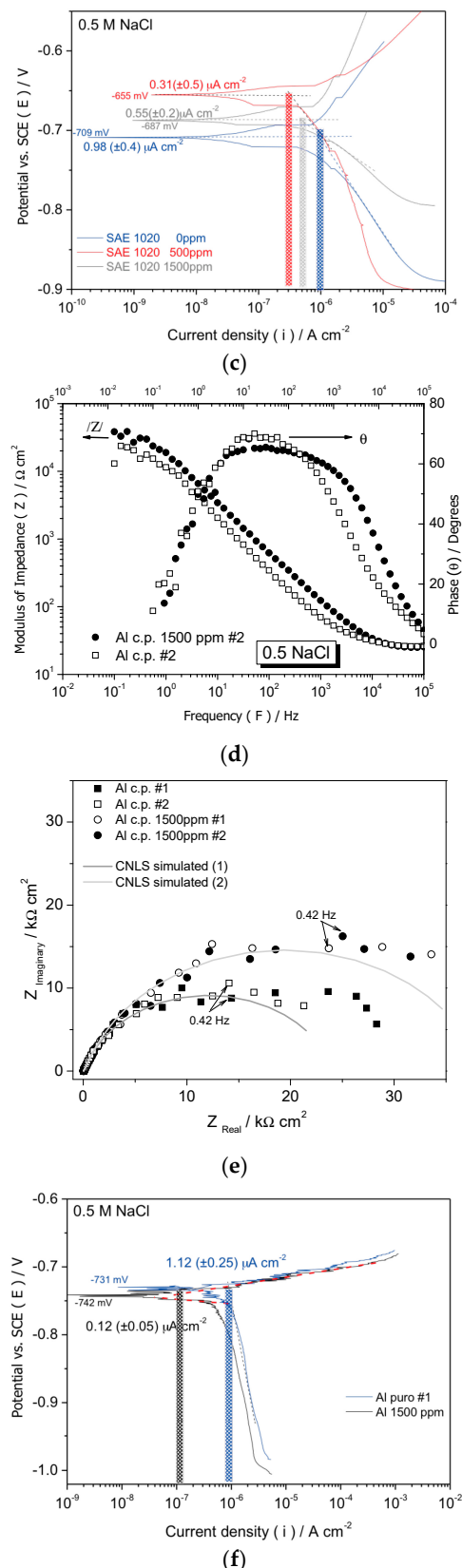


Figure 6. Experimental EIS results and potentiodynamic polarization curves of: (a–c) the SAE 1020 low-carbon steel; and (d–f) the c.p. Al samples in 0.5 M NaCl solution at room temperature.

Once again, it is highlighted that greater details from an electrochemical point of view could be developed, but this is not the focus at this moment.

Table 5 shows EIS parameters of the SAE1020 and c.p. Al samples with distinct DRIMIA contents. Considering the SAE 1020 sample, it can be seen that R_s varies in with the distinct DRIMIA contents. Differently from that variation observed in the Al-Si alloy, which has slightly increased. It seems that cation Fe^{2+} potentially modifies the electrolyte resistance at the sample surface. This seems to be associated with complex intermediate products such as FeOH and/or Fe-chloro and $\text{Fe-chloride-inhibitor}$ molecule complexes, as similarly proposed by Garai et al. [51]. This also seems to contribute with variation of the resistances R_1 and capacitances $Z_{\text{CPE}(1)}$ obtained. It is remembered that R_1 and $Z_{\text{CPE}(1)}$ are the resistance of charge transfer at surface and the capacitance associated with the inner layers on the surface of the examined SAE 1020 and c.p. Al samples, respectively. With this, it is observed that both the SAE 1020 in blank condition and containing 1500 ppm of the inhibitor DRIMIA compound have higher capacitances $Z_{\text{CPE}(1)}$ than the samples with 500 ppm. Additionally, the capacitances $Z_{\text{CPE}(2)}$ are higher for the blank and containing 1500 ppm than the sample with 500 ppm. The resistances R_2 for the samples containing DRIMIA content also suggest that the inhibitor provides a higher R_2 with increased inhibitor concentration, as can be seen in Table 5. These quantitative EIS parameters are also intimately associated with those results suggested by PP curves, i.e., the lowest corrosion current density is that of the sample with 500 ppm.

Table 5. Experimental impedance parameters of the SAE1020 and c.p. Al samples in a 0.5 M NaCl solution with different DRIMIA compound contents by using CNLS simulation and equivalent circuit.

| Parameters (at 25 °C) | SAE1020 | | | c.p. Al | |
|--|----------------------------|------------------------------|------------------------------|------------------------------|------------------------------|
| | 0 ppm | 500 ppm | 1500 ppm | 0 ppm | 1500 ppm |
| $R_s (\Omega \cdot \text{cm}^2)$ | 97(±1) | 162(±2) | 88(±1) | 25(±1) | 23(±0.5) |
| $Z_{\text{CPE}1} (10^{-6} \text{ F/cm}^2)$ | 152.9(±2.5) | 11.38(±0.4) | 69.97(±1.6) | 8.55(±0.2) | 6.89(±1.2) |
| $R_1 (\Omega \cdot \text{cm}^2)$ | 1560(±20) | 583(±75) | 2384(±67) | 85(±14) | 1336(±220) |
| n_1 | 0.69 | 0.86 | 0.77 | 0.84 | 0.82 |
| $Z_{\text{CPE}2} (\text{F/cm}^2)$ | 11.2×10^{-3} (±1) | 7.46×10^{-6} (±0.4) | 1.12×10^{-3} (±0.1) | 6.75×10^{-6} (±0.5) | 2.65×10^{-6} (±0.2) |
| $R_2 (10^3 \Omega \cdot \text{cm}^2)$ | 6.2×10^3 (±0.1) | 15.18 (±0.2) | 8.37 (±1.2) | 24.1 (±0.6) | 37.2 (±0.9) |
| n_2 | 0.81 | 0.86 | 0.59 | 0.81 | 0.85 |
| χ^2 | 1.3×10^{-3} | 5.7×10^{-3} | 1.6×10^{-3} | 10×10^{-3} | 9.1×10^{-3} |
| Sum of Sq. | 0.12 | 0.55 | 0.17 | 0.87 | 0.85 |

When the EIS parameters associated with the c.p. Al samples are observed, all parameters indicate satisfactory inhibition effect. Although the parameters R_s and $Z_{\text{CPE}(1)}$ are very similar, R_2 and $Z_{\text{CPE}(2)}$ parameters favor the sample with inhibitor, i.e., the capacitance $Z_{\text{CPE}(2)}$ substantially decreases ($\sim 2.5 \times$) while R_2 increases by about 1.5 times.

It is worth noting that both the SAE1020 and the c.p. Al samples have demonstrated effective inhibition effects when the DRIMIA contents are utilized. However, a systemic study is always highlighted to find out the best or most ideal ratio (concentration) of the DRIMIA to achieve the best corrosion inhibition efficiency. It can also be said that the 1250 ppm, at room temperature, induces excellent inhibition effects for both the c.p. Al and the Al-7.5%Si alloy samples.

Figure 7a,b shows the experimental results concerning Langmuir and Temkin isotherms with corresponding R^2 (correlation coefficient) and K_{ADS} adsorption coefficients. Only these two isotherms are adopted due to the best quality fittings being attained, i.e., 0.9479 and 0.9432 for the SAE 1020 and c.p. Al samples, considering Langmuir, respectively.

The ΔG_{ads} determined for both the c.p. Al and SAE 1020 are also depicted in Figure 7 considering Langmuir and Temkin isotherms. For all examined cases, all attained ΔG_{ads} are negative values. This suggests spontaneous adsorption of the DRIMIA, as also previously verified when the Al-Si alloys are also examined. Since these values are close to -20 kJ mol^{-1} , physisorption is suggested. With this, as previously discussed, an electrostatic interaction between charged organic molecules and the charged metal surface is prevalent. Based on this, the physisorption mechanism domains the adsorption behavior of DRIMIA

onto the surface of the SAE 1020 and c.p. Al samples. This can also be explained by utilizing Figure 5. Evidently, Al^{3+} and Fe^{+2} and intermediate corrosion by-products differentiate in the schematic representation considering each specific substrate material.

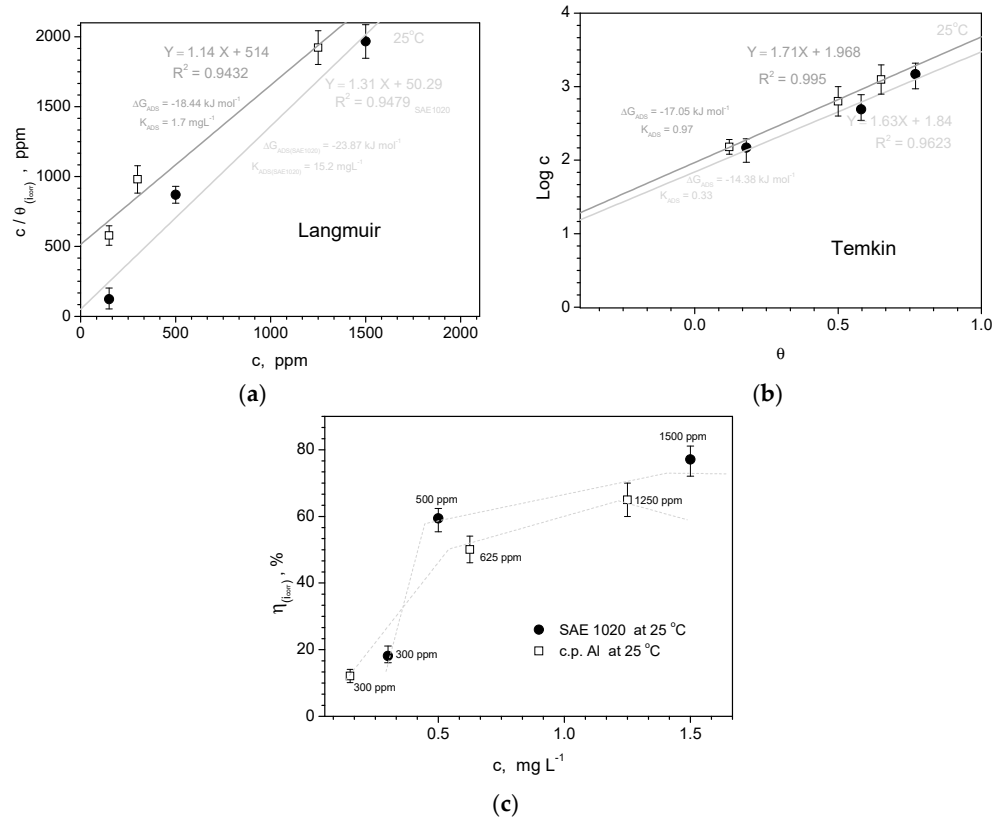


Figure 7. (a) Langmuir, (b) Temkin adsorption isotherms plots at 25 °C; and (c) the resulting inhibition efficiency (in percentages) as a function of the DRIMIA concentrations at 25 °C.

Based on the attained results, it is suggested that there exists adequate DRIMIA content to be used for each particular situation, considering each distinct material. As an example of this, Table 6 depicts a summary of the inhibition percentage values for the materials evaluated at room temperature and the respective concentrations applied. Based on these data, it is clear that careful attention must be given to the concentration of the inhibitor to be used. It is observed that for the same order of magnitude of inhibitor content for the three different materials (between 1250 and 1500 ppm), the highest inhibition efficiency is that of the Al-Si alloy, which has reached about 96%. Although no systematic evaluation for the SAE 1020 samples is provided, it is suggested that lower DRIMIA concentrations will provide better inhibitor efficiency. However, this is merely speculative, because in the present investigation with SAE1020, the aim is only to verify if DRIMIA also provides an inhibition effect when added to an aggressive NaCl solution. An analog conclusion can also be provided when the c.p. Al samples are evaluated.

In a general and limited comparison, when 1/3 of the concentration of inhibitor is used for aluminum alloy and steel, the efficiencies respond substantially and distinctively. Although it is believed that adsorption and inhibition mechanisms are very similar, it is also suggested that the DRIMIA content potentially prevents or protects the material in distinctive concentrations when different materials are considered. For the Al-Si alloy, the use of 2× more concentration resulted in slight increasing (~2%) in terms of the attained efficiency level. On the other hand, with a triple concentration for steel, the efficiency decreased considerably (~20%). This indicates that although an inhibitory effect on the three materials is achieved, the concentration has a specific “sensitivity” for each material, which suggests meticulous planning in its dosage.

Table 6. Comparisons among percentages of inhibition efficiencies (IE or η) provided by DRIMIA at environmental temperature for the c.p. Al, Al-Si casting alloy, and SAE 1020 low-carbon steel samples.

| Concentration (ppm) | Examined Material | η (%) |
|---------------------|-------------------|-------------------|
| 1250 | c.p. Al | ~89 (± 2) |
| 1250 | Al-Si alloy | ~96 (± 1.5) |
| 625 | | ~94 (± 1.5) |
| 500 | SAE 1020 | ~68 (± 5) |
| 1500 | | ~44 (± 3) |

4. Conclusions

Based on the obtained results of the corrosion behavior using potentiodynamic polarization curves and electrochemical impedance spectroscopy carried out in distinctive SAE steel, pure Al, and Al-Si alloy samples in a 0.5 M NaCl solution using *Drimia maritima* as a green inhibitor, the following summarized conclusions can be drawn:

- When as-cast Al-Si alloy samples are evaluated by using potentiodynamic polarization curves, both IE% (inhibition efficiency percentage) and θ (surface coverage) results have demonstrated ~96% and 0.96 are attained, respectively. This is when a *Drimia maritima* concentration of 1250 ppm is used. When 1875 ppm is applied, the corrosion current density increases, which demonstrates that efficiency is negatively affected. It is important to remark that when 150 ppm is utilized, the IE% and θ have only achieved ~47% and 0.47, respectively. These aforementioned results correspond with solutions at environmental temperature (~25 °C). However, when at a higher temperature (~45 °C), *Drimia maritima* green inhibitor also demonstrated a positive effect, attaining about 43% when 625 ppm is utilized.
- When EIS results are also evaluated, similar trends concerning the inhibition effect are observed, i.e., the highest inhibition is that of 1250 ppm at 25 °C and 625 ppm at 45 °C. These assertions are achieved when capacitances and their corresponding polarization resistances are examined.
- When both SAE steel and commercially pure Al samples are also examined, it is also verified that inhibition effects are provided. Considering the SAE steel sample, the highest IE% is that of 500 ppm of *Drimia maritima*. On the other hand, when c.p. Al samples are examined, the concentration of *Drimia maritima* that provides the highest inhibition behavior (~89%) is that of 1250 ppm. Similar trends are also reached when EIS data are examined.
- Based on the determined isothermal adsorption plots by using distinctive methods (i.e., Langmuir, Temkin, Frumkin, Flory-Huggins, and Freundlich isotherm), the obtained parameters have indicated that a physical adsorption mechanism is prevalent on all examined samples. With this, it is considered that an electrostatic interaction (physisorption) mechanism domains the adsorption between negatively charged of the DRIMIA components positively charged cation of “metal” (Al or Fe) at surface.
- Finally, although it is found that physisorption domains affect the inhibition behavior of the three distinctive materials, it is confirmed that different concentrations provide distinct protection levels or inhibition into NaCl solution. For instance, in the Al-Si alloy, the use of 1250 ppm attains an efficiency level of about 96%, while for the c.p. Al sample, only 89% is achieved. On the other hand, the SAE steel sample has its efficiency decreased to ~44%. This indicates that the dosage of *Drimia maritima* content as a green inhibitor into NaCl solution shows certain “susceptibility” for each examined material and should be carefully planned in order to obtain the maximum inhibitor behavior without deleterious and catastrophic effects.

Author Contributions: R.S.B., D.C. and G.S.P. elaborated solution and prepared the samples/specimens; D.C., A.D.B. and W.R.O. carried out the corrosion evaluations/measurements, organized the data,

and correlated with attained results of all examined specimens; A.D.B. and W.R.O. also contributed to the general organization and English writing. All authors have read and agreed to the published version of the manuscript.

Funding: The financial support provided by FAEPEX-UNICAMP (#2091/24), CAPES (Coordination for the Improvement of Higher Education Personnel), Ministry of Education, Brazil, Grant #1) and CNPq (The Brazilian Research Council) Grants, 402704/2023-1, 407595/2022-8; #313272/2021-2.

Institutional Review Board Statement: Not applicable.

Informed Consent Statement: Not applicable.

Data Availability Statement: All research data supporting this publication are directly available within this publication.

Acknowledgments: Acknowledgments are also provided to Luiz Antonio Garcia (technician department) who has contributed with technical aspects and equipment organization.

Conflicts of Interest: The authors declare no conflicts of interest.

References

1. Schweitzer Philip, A. *Corrosion Engineering Handbook*, 1st ed.; CR Press: Winston-Salem, NC, USA, 1996.
2. Schweitzer Philip, A. *Metallic Materials: Physical, Mechanical, and Corrosion Properties (Corrosion Technology)*, 1st ed.; CR Press: Winston-Salem, NC, USA, 2006.
3. Wolynec, S. *Técnicas Eletroquímicas em Corrosão*; EDUSP—Editora Universidade de São Paulo: São Paulo, Brazil, 2003.
4. Paul, L.; Machunda, R.L. Investigation of Aloe lateritia Gel as Corrosion Inhibitor for Mild Steel in 2 M HNO₃ and 1 M H₂SO₄ Media. *J. Miner. Mater. Charact. Eng.* **2016**, *4*, 33–39.
5. Kesavan, D.; Gopiraman, M.; Sulochana, N. Green Inhibitors for Corrosion of Metals: A Review. *Chem. Sci. Rev. Lett.* **2012**, *1*, 1–8.
6. Koch, G.H.; Brongers, M.P.H.; Thompson, N.G.; Virmani, Y.P.; Payer, J.H. *Corrosion Costs and Preventive Strategies in the United States*; NACE Intl PHWA-RD-01-156; NACE International: Houston, TX, USA, 2002.
7. Khadraoui, A.; Khelifa AHamitouche, H.; Mehdaoui, R. Inhibitive effect by extract of *Mentha rotundifolia* leaves on the corrosion of steel in 1 M HCl solution. *Res. Chem. Intermed.* **2014**, *40*, 961–972. [[CrossRef](#)]
8. Xhanari KFinsgar, M.; Hrnacic, M.K.; Maver, U.; Kneza, Z.; Seiti, B. Green corrosion inhibitors for aluminium and its alloys: A review. *R. Soc. Chem. RSC Adv.* **2017**, *7*, 27299–27330. [[CrossRef](#)]
9. Inzunza, R.G.; Valdez, B.; Schorr, M. Corrosion Inhibitor Patents in Industrial Applications—A Review. *Recent Pat. Corros. Sci.* **2013**, *3*, 71–78. [[CrossRef](#)]
10. Hart, K.; James, A.O. The Inhibitive Effect of Aloe Vera Barbadensis Gel on Copper in Hydrochloric Acid Medium. *J. Emerg. Trends Eng. Appl. Sci. JETEAS* **2014**, *5*, 24–29.
11. Abiola, O.K.; Oforka, N.C. The corrosion inhibition of Azadirachta leaves extract on corrosion of mild steel in HCl solution. *Mater. Chem. Phys.* **2002**, *70*, 241–268.
12. Sangeetha, M.; Rajendran, S.; Sathiyabama, J.; Krishnavenic, A. Inhibition of Corrosion of Aluminium and its Alloys by Extracts of Green Inhibitors. *Port. Electrochim. Acta* **2013**, *31*, 41–52. [[CrossRef](#)]
13. Xhanari, K.; Finsgar, M. Organic corrosion inhibitors for aluminium and its alloys in acid solutions: A review. *RSC Adv.* **2016**, *6*, 62833–62857. [[CrossRef](#)]
14. Hatch, E. *Aluminum: Properties and Physical Metallurgy*; ASM International: Almere, The Netherlands, 1984; p. 433.
15. Davis, J.R. *Corrosion of Aluminum and Aluminum Alloys*; ASM International: Almere, The Netherlands, 1999; p. 327.
16. Rodic, P.; Milosevz, I. Inhibition of pure aluminium and alloys AA2024-T3 and AA7075-T6 by cerium(III) and cerium(IV) salts. *J. Electrochem. Soc.* **2016**, *3*, C85–C93. [[CrossRef](#)]
17. Badawy, W.A.; Al-Kharafi, F.M.; El-Azab, A.S. Electrochemical behaviour and corrosion inhibition of Al, Al-6061 and Al-Cu in neutral aqueous solutions. *Corros. Sci.* **1999**, *41*, 709–727. [[CrossRef](#)]
18. Osório, W.R.; Freire, C.M.; Garcia, A. The Role of Macrostructural Morphology and Grain Size on the Corrosion Resistance of Zn and Al Castings. *Mater. Sci. Eng. A* **2005**, *402*, 22–32. [[CrossRef](#)]
19. Osório, W.R.; Moutinho, D.J.; Peixoto, L.C.; Ferreira, I.L.; Garcia, A. Macrosegregation and Microstructure Dendritic Array Affecting the Electrochemical Behaviour of Ternary Al–Cu–Si Alloys. *Electrochim. Acta* **2011**, *56*, 8412–8421. [[CrossRef](#)]
20. Osório, W.R.; Siqueira, C.A.; Santos, C.A.; Garcia, A. The Correlation between Electrochemical Corrosion Resistance and Mechanical Strength of As-Cast Al-Cu and Al-Si Alloys. *Int. J. Electrochem. Sci.* **2011**, *6*, 6275–6289. [[CrossRef](#)]
21. Osório, W.R.; Cheung, N.; Spinelli, J.E.; Goulart, P.R.; Garcia, A. Effects of a eutectic modifier on microstructure and surface corrosion behavior of Al-Si hypoeutectic alloys. *J. Solid State Electrochem.* **2007**, *11*, 1421–1427. [[CrossRef](#)]
22. Osório, W.R.; Freitas, E.S.; Garcia, A. Corrosion Performance Based on the Microstructural Array of Al-Based Monotectic Alloys in a NaCl Solution. *J. Mater. Eng. Perform.* **2014**, *23*, 333–341. [[CrossRef](#)]
23. Osório, W.R.; Canté, M.V.; Brito, C.; Freitas, E.S.; Garcia, A. Electrochemical Behavior of An Al-Fe-Ni Alloy Affected by Nano-Sized Intermetallic Particles. *Corrosion* **2015**, *71*, 510–522. [[CrossRef](#)]

24. Speller, F.N.; Chappel, E.L.; Russell, R.P. Practical applications of inhibitors for pickling operations. *Trans. Am. Inst. Chem. Engrs.* **1927**, *49*, 165–169.
25. Sharma, S.K.; Peter, A.; Obot, I.B. Potential of *Azadirachta indica* as a green corrosion inhibitor against mild steel, aluminum, and tin: A review. *J. Anal. Sci. Technol.* **2015**, *6*, 26–42. [[CrossRef](#)]
26. Obot, I.B.; Obi-Egbedi, N.O. *Ipomoea Involuta* as an Ecofriendly inhibitor for aluminium alkaline medium. *Port. Electrochem. Acta* **2009**, *27*, 517–524. [[CrossRef](#)]
27. Obot, I.B.; Obi-Egbedi, N.O. Ginseng Root: A new Efficient and Effective Eco-Friendly Corrosion Inhibitor for Aluminium Alloy of type AA 1060 in Hydrochloric Acid Solution. *Int. J. Electrochem. Sci.* **2009**, *4*, 1277–1288. [[CrossRef](#)]
28. Badawi, A.K.; Fahim, I.S. A critical review on green corrosion inhibitors based on plant extracts: Advances and potential presence in the market. *Int. J. Corros. Scale Inhib.* **2021**, *10*, 1385–1406.
29. Bashir, S.; Abas, S.; Khan, A.; Gilani, A.H. Studies on bronchodilator and cardiac stimulant activities of *Urninea indica*. *Bangladesh J. Pharmacol.* **2013**, *8*, 249–254. [[CrossRef](#)]
30. Sharma, H.J.; Devi, N.S. Phytochemical Analysis of *Drimia* Species. *Int. J. Appl. Sci.-Res. Rev.* **2017**, *4*, 12.
31. Nejatbakhsh, F.; Karegar-Borzia, H.; Amin, G.; Eslaminejad, A.; Hosseini, M.; Bozorgie, M.; Gharabaghi, M.A. Squill Oxymel, a traditional formulation from *Drimia maritima* (L.) Stearn, as an add-on treatment in patients with moderate to severe persistent asthma: A pilot, triple-blind, randomized clinical trial. *J. Ethnopharmacol.* **2017**, *196*, 186–192. [[CrossRef](#)] [[PubMed](#)]
32. Hamouda, A.B.; Chaieb, I.; Zouari, L.; Zarrad, K.; Laarif, A. Toxicological effects of *Urginea maritima* (L.) against the red flour beetle (Coleoptera: Tenebrionidae). *J. Entomol. Zool. Stud.* **2016**, *4*, 17–20.
33. Gould, L.; Fisch, S.; Cherbakoff, A.; Degriff, A.C. Clinical studies on proscillarin A, a new squill glycoside. *J. Clin. Pharmacol. New Drugs* **1971**, *11*, 135–145. [[CrossRef](#)]
34. Bielawski, K.; Winnicka, K.; Bielawska, A. Inhibition of DNA topoisomerases I and II, and growth inhibition of breast cancer MCF-7 cells by ouabain, digoxin and proscillarin A. *Biol. Pharm. Bull.* **2006**, *29*, 1493–1497. [[CrossRef](#)] [[PubMed](#)]
35. Winnicka, K.; Bielawski, K.; Bielawska, A.; Miltyc, W. Apoptosis-mediated cytotoxicity of ouabain, digoxin and proscillarin A in the estrogen independent MDA-MB-231 breast cancer cells. *Arch. Pharm. Res.* **2007**, *30*, 1216–1224. [[CrossRef](#)]
36. Nilubol, N.; Zhang, L.; Shen, M.; Zhang, Y.Q.; He, M.; Austin, C.P.; Kebebew, E. Four clinically utilized drugs were identified and validated for treatment of adrenocortical cancer using quantitative high-throughput screening. *J. Transl. Med.* **2012**, *10*, 198. [[CrossRef](#)]
37. Rugmini Ammal, P.; Prajila, M.; Joseph, A. Physicochemical studies on the inhibitive properties of a 1,2,4-triazole Schiff's base, HMATD, on the corrosion of mild steel in hydrochloric acid. *Egypt. J. Pet.* **2017**, *27*, 307–317. [[CrossRef](#)]
38. Obi-Egbedi, N.O.; Obot, I.B.; Umoren, S.A. *Spondias mombin* L. as a green corrosion inhibitor for aluminium in sulphuric acid: Correlation between inhibitive effect and electronic properties of extracts major constituents using density functional theory. *Arab. J. Chem.* **2012**, *5*, 361–373. [[CrossRef](#)]
39. Wang, C.; Zou, C.; Cao, Y. Electrochemical and isothermal adsorption studies on corrosion inhibition performance of β -cyclodextrin grafted polyacrylamide for X80 steel in oil and gas production. *J. Mol. Struct.* **2021**, *1228*, 129737. [[CrossRef](#)]
40. Hirschorn, B.; Orazem, M.E.; Tribollet, B.; Vivier, V.; Frateur, I.; Musiani, M. Determination of effective capacitance and film thickness from constant-phase-element parameters. *Electrochim. Acta* **2010**, *55*, 6218–6227. [[CrossRef](#)]
41. Orazem, M.E.; Pébère, N.; Tribollet, B. Enhanced Graphical Representation of Electrochemical Impedance. *J. Electrochem. Soc.* **2006**, *153*, 129–136. [[CrossRef](#)]
42. Al-Abdallat, K.; Obeidat, M.; Ababneh, N.A.; Zalloum, S.; Al Hadidi, S.; Al-Abdallat, Y.; Zihlif, M.; Awidi, A. Phytochemical analysis and anticancer properties of *Drimia maritima* bulb extracts on colorectal cancer cells. *Molecules* **2023**, *28*, 1215. [[CrossRef](#)]
43. Meyer, Y.A.; Menezes, I.; Bonatti, R.S.; Bortolozo, A.D.; Osório, W.R. EIS Investigation of the Corrosion Behavior of Steel Bars Embedded into Modified Concretes with Eggshell Contents. *Metals* **2022**, *12*, 417. [[CrossRef](#)]
44. Duarte, T.; Meyer, Y.A.; Osório, W.R. The Holes of Zn Phosphate and Hot Dip Galvanizing on Electrochemical Behaviors of Multi-Coatings on Steel Substrates. *Metals* **2022**, *12*, 863. [[CrossRef](#)]
45. Lai, X.; Hu, J.; Ruan, T.; Zhou, J.; Qu, J. Chitosan derivative corrosion inhibitor for aluminum alloy in sodium chloride solution: A green organic/inorganic hybrid. *Carbohydr. Polym.* **2021**, *265*, 118074. [[CrossRef](#)]
46. Nazir, U.; Akhter, Z.; Ali, N.Z.; Shah, F.U. Experimental and theoretical insights into the corrosion inhibition activity of novel Schiff bases for aluminum alloy in acidic medium. *RSC Adv.* **2019**, *9*, 36455–36470. [[CrossRef](#)]
47. Jakeria, M.R.; Toh, R.J.; Che, X.B.; Cole, I.S. Evolution and stability of 2-mercaptopbenzimidazole inhibitor film upon Al alloy 6061. *J. Appl. Electrochem.* **2022**, *52*, 1021–1044. [[CrossRef](#)]
48. Wang, J.; Zhao, J.; Tabish, M.; Peng, L.; Cheng, Q.; Shi, F. Long-term corrosion inhibition fro AA5052 aluminum alloy by an eco-friendly hybrid inhibitor: Synergism inhibition between rosemary extract and zinc chloride in 0.05M NaCl solution. *J. Ind. Eng. Chem.* **2023**, *120*, 302–315. [[CrossRef](#)]
49. Farag, A.A.; Ismail, A.S.; Migahed, M.A. Squid By-product Gelatin Polymer as an Eco-friendly Corrosion Inhibitor for Carbon Steel in 0.5 M H₂SO₄ Solution: Experimental, Theoretical, and Monte Carlo Simulation Studies. *J. Bio-Tribos-Corros.* **2020**, *6*, 16. [[CrossRef](#)]

50. Pradityana ASulistijono, A.; Shahab, A.; Noerochim, L.; Susanti, D. Inhibition of Corrosion of Carbon Steel in 3.5% NaCl Solution by *Myrmecodia pendans* Extract. *Int. J. Corros.* **2016**, *2016*, 6058286. [[CrossRef](#)]
51. Garai, S.; Garai, S.; Jaisankar, P.; Singh, J.K.; Elango, A. A comprehensive study on crude methanolic extract of *Artemisia pallens* (Asteraceae) and its active component as effective corrosion inhibitors of mild steel in acid solution. *Corros. Sci.* **2012**, *60*, 193–204. [[CrossRef](#)]

Disclaimer/Publisher's Note: The statements, opinions and data contained in all publications are solely those of the individual author(s) and contributor(s) and not of MDPI and/or the editor(s). MDPI and/or the editor(s) disclaim responsibility for any injury to people or property resulting from any ideas, methods, instructions or products referred to in the content.